Status of the DMRadio Program

Nicholas Rapidis

Stanford University – Irwin Group

DMRadio Collaboration

Shoot for the Stars, Aim for the Axions – October 6, 2022

DMRadio Collaboration

H.M. Cho, W. Craddock, D. Li, C. P. Salemi, W. J. Wisniewski
SLAC National Accelerator Laboratory

J. Corbin, P. W. Graham, K. D. Irwin, F. Kadribasic, S. Kuenstner, N. M. Rapidis, M. Simanovskaia, J. Singh, E. C. van Assendelft, K. Wells
Department of Physics
*Stanford University – **Experiment Location***

A. Droster, A. Keller, A. F. Leder, K. van Bibber
Department of Nuclear Engineering
University of California Berkeley

S. Chaudhuri, R. Kolevatov
Department of Physics
Princeton University

L. Brouwer
Accelerator Technology and Applied Physics Division
Lawrence Berkeley National Lab

B. A. Young
Department of Physics
Santa Clara University

J. W. Foster, J. T. Fry, J. L. Ouellet, K. M. W. Pappas, L. Winslow
Laboratory of Nuclear Science
Massachusetts Institute of Technology

R. Henning
Department of Physics
University of North Carolina Chapel Hill
Triangle Universities Nuclear Laboratory

Y. Kahn
Department of Physics
University of Illinois at Urbana-Champaign

A. Phipps
California State University, East Bay

B. R. Safdi
Department of Physics
University of California Berkeley

Outline

1. Axions and low frequency haloscopes
2. DMRadio 50L
    1. Overview
    2. Status
3. DMRadio m^3
    1. Overview
    2. Status
4. Outlook, future, & collaboration

Outline

1. Axions and low frequency haloscopes
2. DMRadio 50L
    1. Overview
    2. Status
3. DMRadio m^3
    1. Overview
    2. Status
4. Outlook, future, & collaboration

Axions

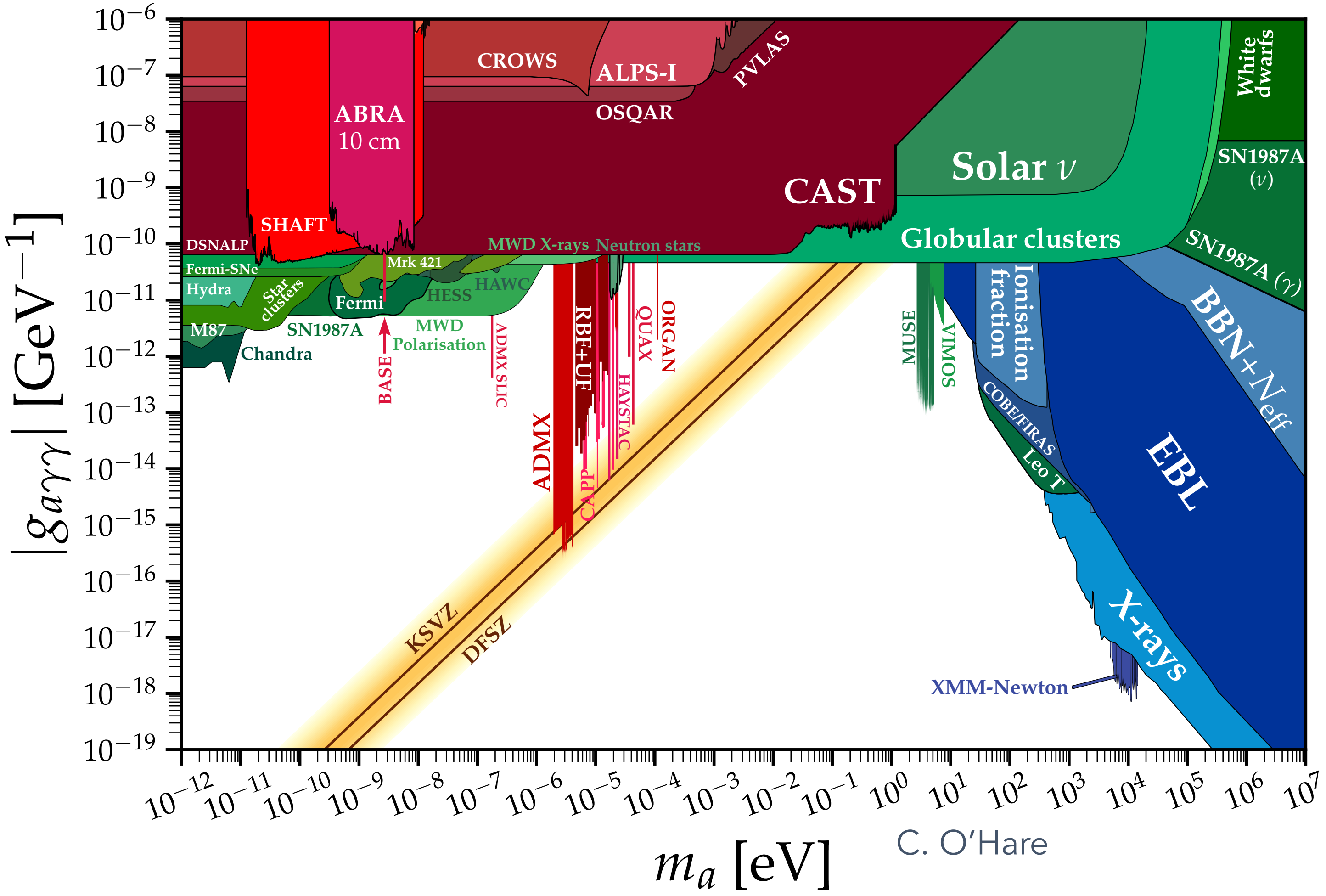

C. O'Hare

Axions

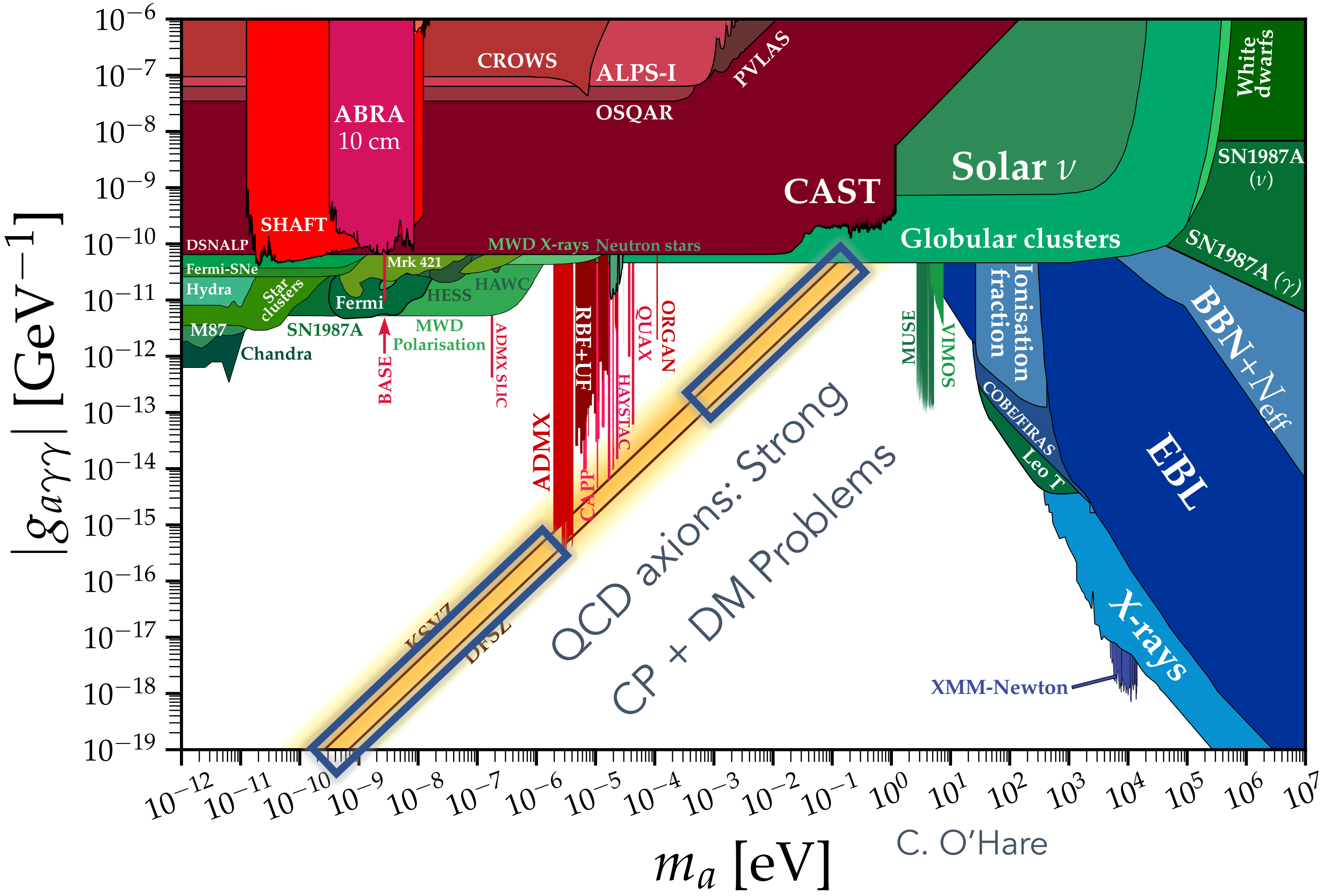

CROWS
ALPS-I
PVLAS
ABRA
10 cm
OSQAR
SHAFT
CAST
Solar ν
White dwarfs
SN1987A (ν)
DSNALP
MWD X-rays
Neutron stars
Globular clusters
SN1987A (γ)
Fermi-SNe
Mrk 421
Hydra
Star clusters
Fermi
HESS
HAWC
M87
SN1987A
MWD Polarisation
Chandra
BASE
ADMX SLIC
ADMX
RBF+UF
CAPP
HAYSTAC
QUAX
ORGAN
MUSE
VIMOS
Ionisation fraction
BBN+N_{eff}
COBE/FIRAS
Leo T
EBL
X-rays
XMM-Newton
KSVZ
DFSZ
QCD axions: Strong
CP + DM Problems
$|g_{a\gamma\gamma}|$ [GeV^{-1}]
m_a [eV]
C. O'Hare

Axions

Axion to photon conversion:

$$\nu_a = \frac{m_a c^2}{h}$$

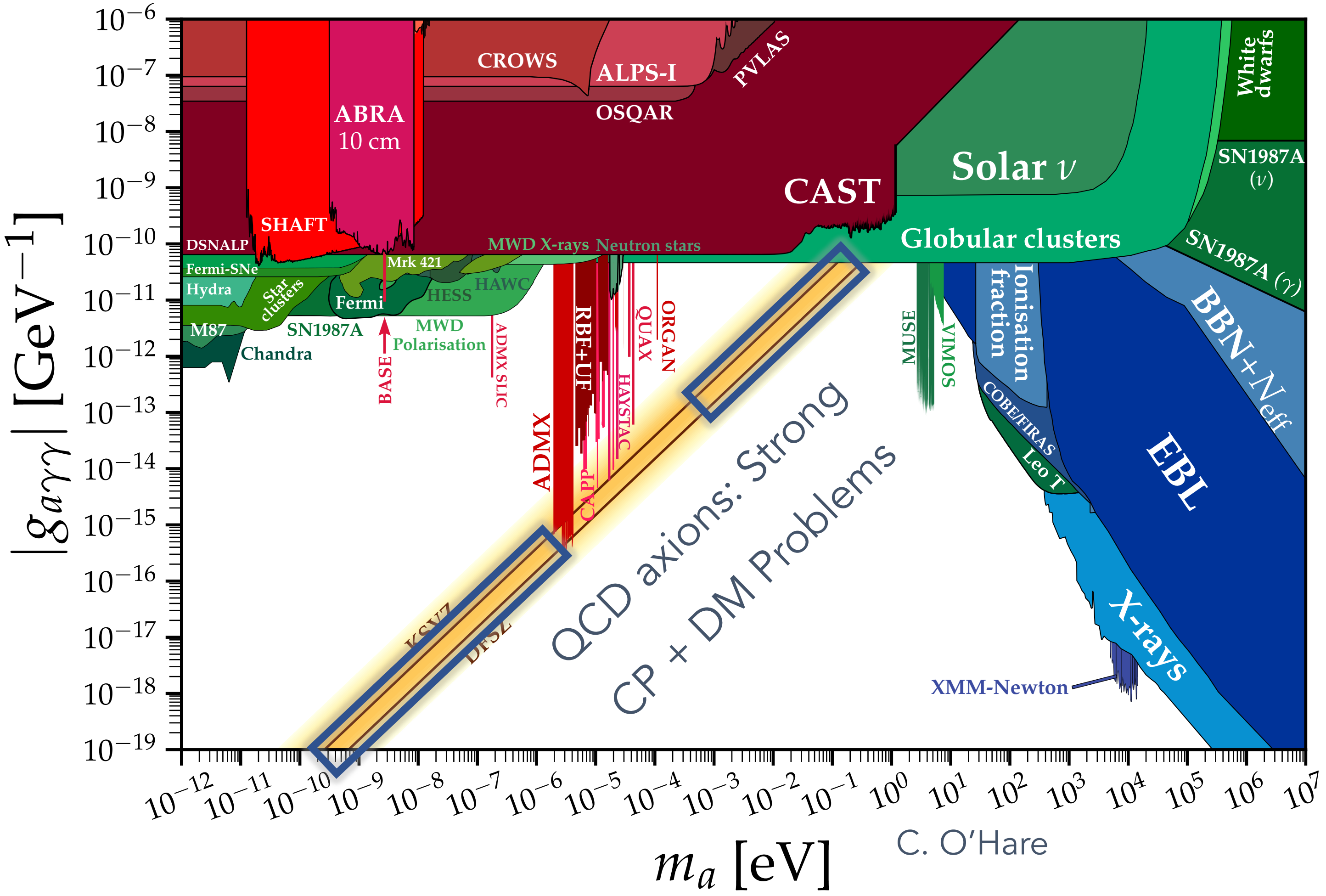

Axions

Axion to photon conversion:

$$\nu_a = \frac{m_a c^2}{h}$$

QCD axion symmetry breaking scale:

$$f_a \sim g_{a\gamma\gamma}^{-1}$$

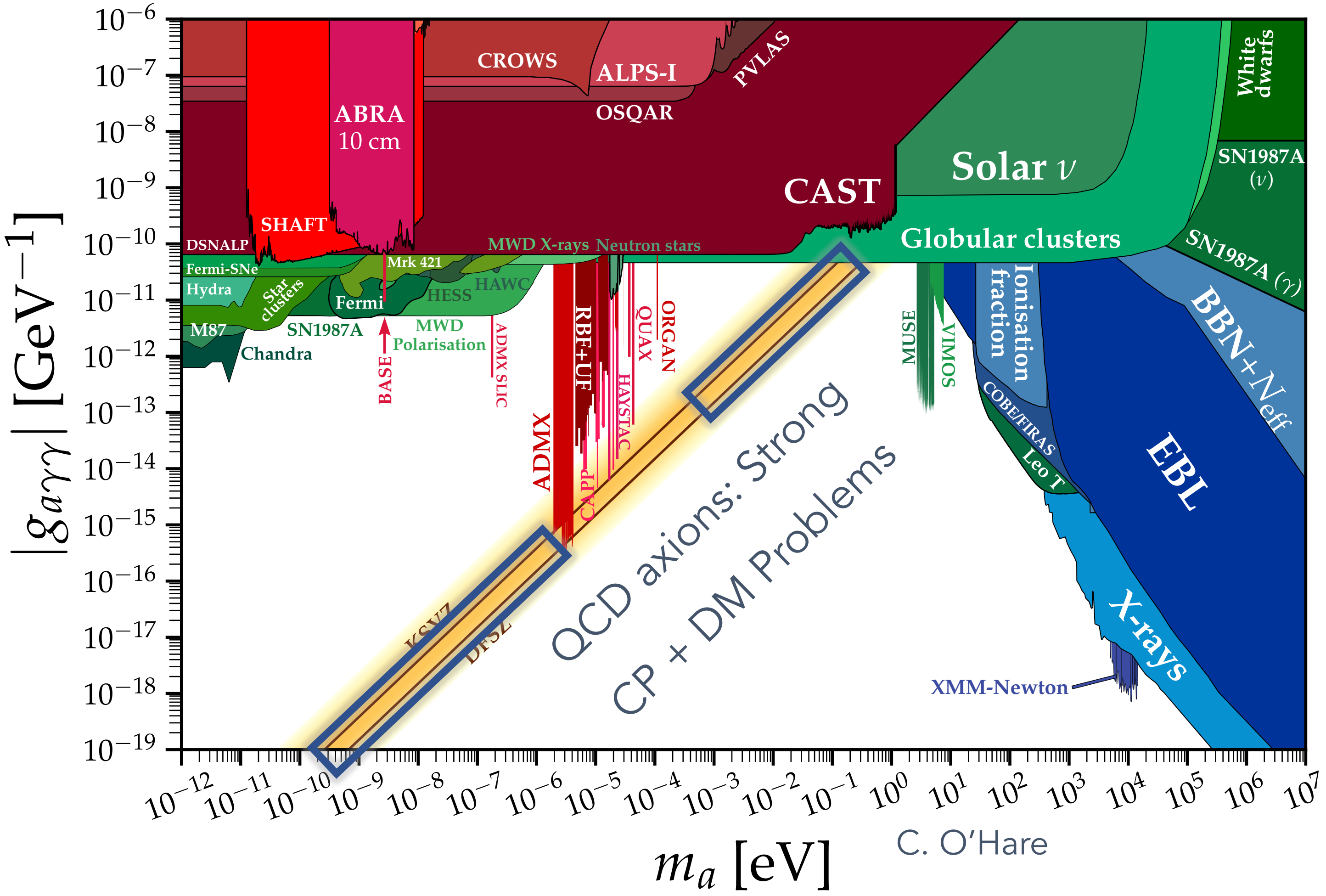

Axions

Axion to photon conversion:

$$\nu_a = \frac{m_a c^2}{h}$$

QCD axion symmetry breaking scale:

$$f_a \sim {g_{a\gamma\gamma}}^{-1}$$

Axion parameter space is well motivated for:

$$\Lambda_{\text{inflation}} < f_a \lesssim m_{\text{Planck}}$$

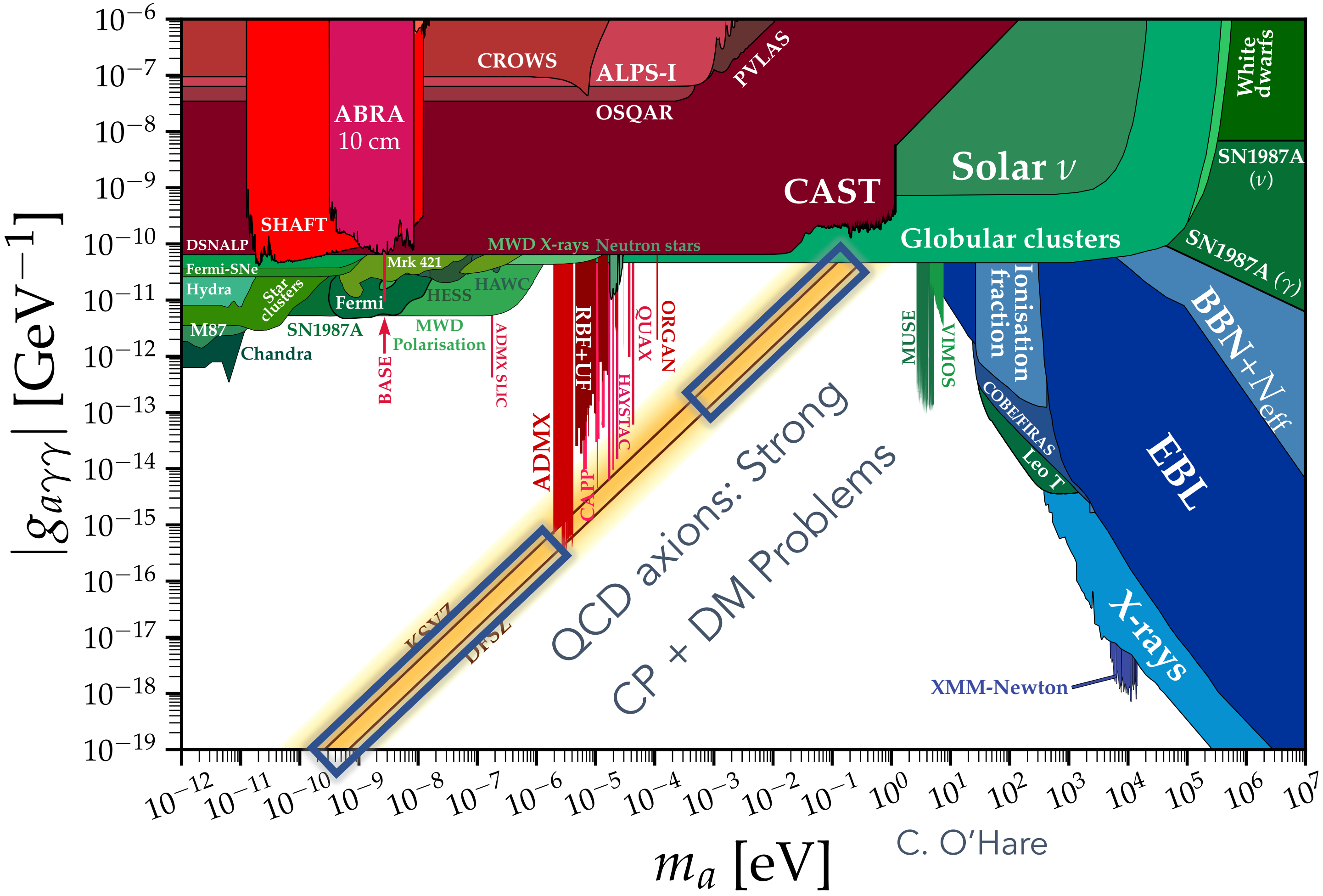

Graham and Scherlis, arXiv: 1805.07362

Axions and Axion DM

Axion-photon coupling:

$$\mathcal{L} \supset g_{a\gamma\gamma} a F\tilde{F} \sim g_{a\gamma\gamma} a \vec{E} \cdot \vec{B}$$

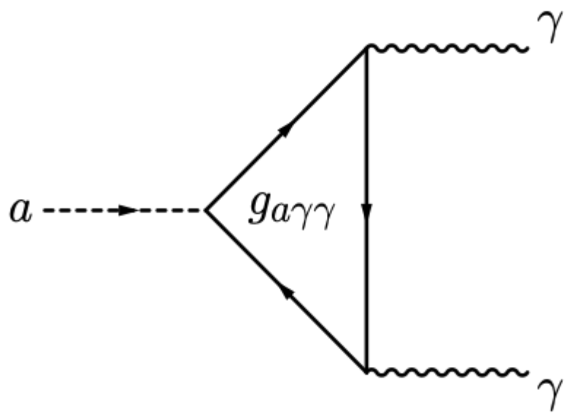

Axions and Axion DM

Axion-photon coupling:

$$\mathcal{L} \supset g_{a\gamma\gamma} a F\tilde{F} \sim g_{a\gamma\gamma} a \vec{E} \cdot \vec{B}$$

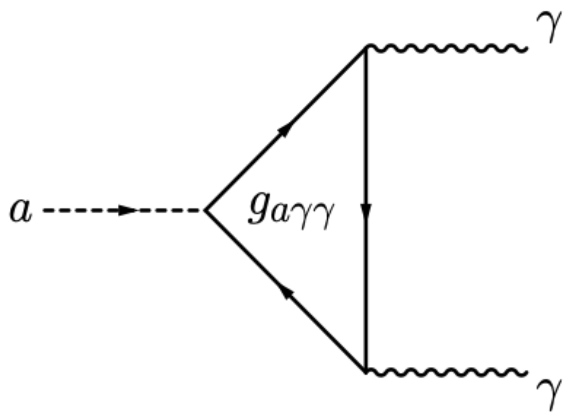

For axion haloscopes:

Axion + magnetic field photon

→ electric field photon

Axions and Axion DM

Axion-photon coupling:

$$\mathcal{L} \supset g_{a\gamma\gamma} a F\tilde{F} \sim g_{a\gamma\gamma} a \vec{E} \cdot \vec{B}$$

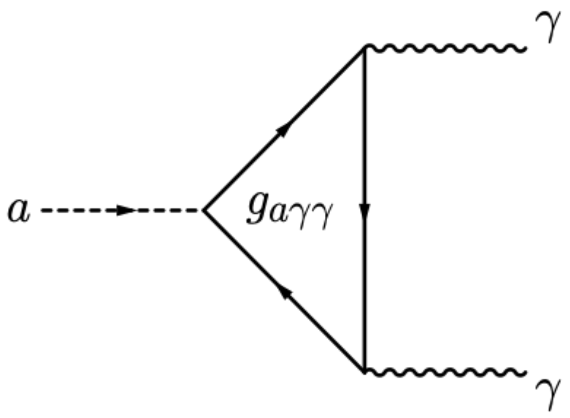

For axion haloscopes:

Axion + magnetic field photon

→ electric field photon

Expected axion number density (for neV axion)

$$n_a \sim 10^{17} \text{cm}^{-3} \gg 1 \quad \text{per quantum state}$$

Axion can be modeled as classical wave

Axions and Axion DM

Axion-photon coupling:

$$\mathcal{L} \supset g_{a\gamma\gamma} a F\tilde{F} \sim g_{a\gamma\gamma} a \vec{E} \cdot \vec{B}$$

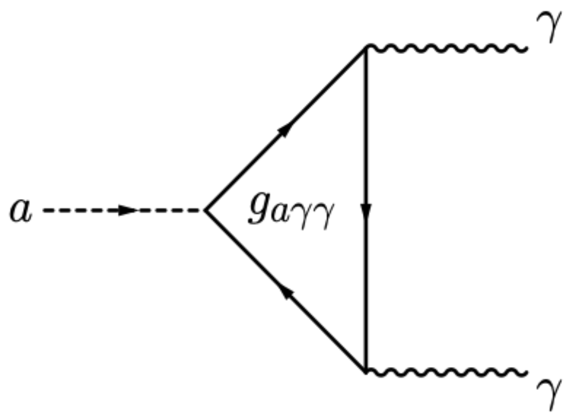

For axion haloscopes:

Axion + magnetic field photon

→ electric field photon

Expected axion number density (for neV axion)

$$n_a \sim 10^{17}\text{cm}^{-3} \gg 1 \quad \text{per quantum state}$$

Axion can be modeled as classical wave

$$\nabla \cdot \vec{E} = -g_{a\gamma\gamma} \vec{B} \cdot \nabla a$$
$$\nabla \cdot \vec{B} = 0$$
$$\nabla \times \vec{E} = -\partial_t \vec{B}$$
$$\nabla \times \vec{B} = \partial_t \vec{E} - g_{a\gamma\gamma} \left(\vec{E} \times \nabla a - \partial_t a \vec{B} \right)$$

Axions and Axion DM

Axion-photon coupling:

$$\mathcal{L} \supset g_{a\gamma\gamma} a F \tilde{F} \sim g_{a\gamma\gamma} a \vec{E} \cdot \vec{B}$$

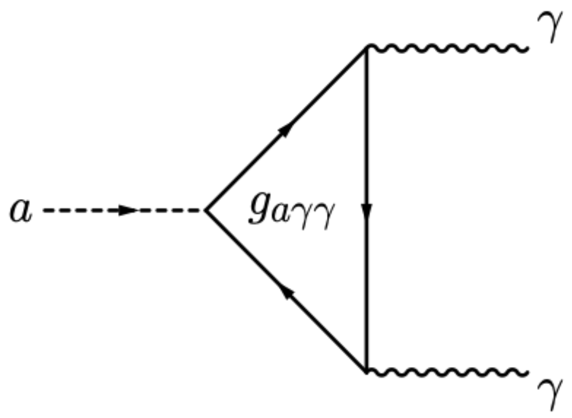

For axion haloscopes:

Axion + magnetic field photon

→ electric field photon

Expected axion number density (for neV axion)

$n_a \sim 10^{17} \mathrm{cm}^{-3} \gg 1$ per quantum state

Axion can be modeled as classical wave

$$\nabla \cdot \vec{E} = -g_{a\gamma\gamma} \vec{B} \cdot \nabla a$$
$$\nabla \cdot \vec{B} = 0$$
$$\nabla \times \vec{E} = -\partial_t \vec{B}$$
$$\nabla \times \vec{B} = \partial_t \vec{E} - g_{a\gamma\gamma} \left(\vec{E} \times \nabla a - \boxed{\partial_t a \vec{B}} \right)$$

$$\vec{J}_{\text{eff}} = g_{a\gamma\gamma} \partial_t a \vec{B}$$

Axion Parameter Space

$$\vec{J}_{\text{eff}} = g_{a\gamma\gamma}\partial_t a\vec{B}$$

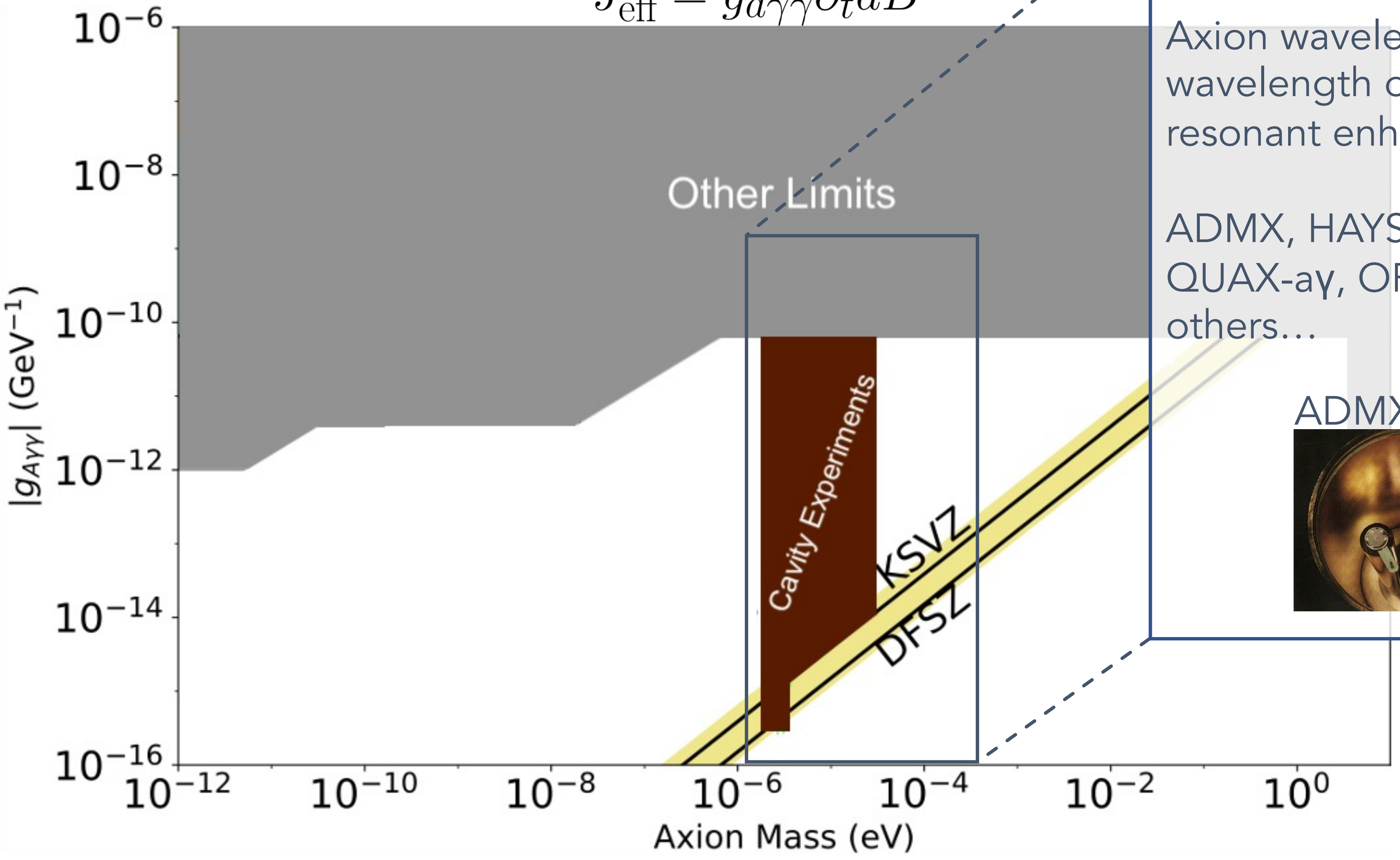

Wavelength $\lambda \lesssim 1$ m

Axion wavelength matches wavelength of cavity mode – resonant enhancement

ADMX, HAYSTAC, CAPP-8TB, QUAX-aγ, ORGAN, MADMAX, others…

ADMX

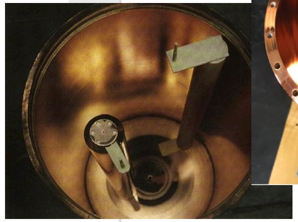

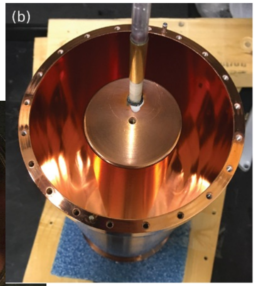

HAYSTAC

Axion Parameter Space

$$\vec{J}_{\text{eff}} = g_{a\gamma\gamma}\partial_t a\vec{B}$$

Wavelength $\lambda \gg 1\ \text{m}$

Axion frequency matches resonance of LC oscillator

Pre-inflationary axion

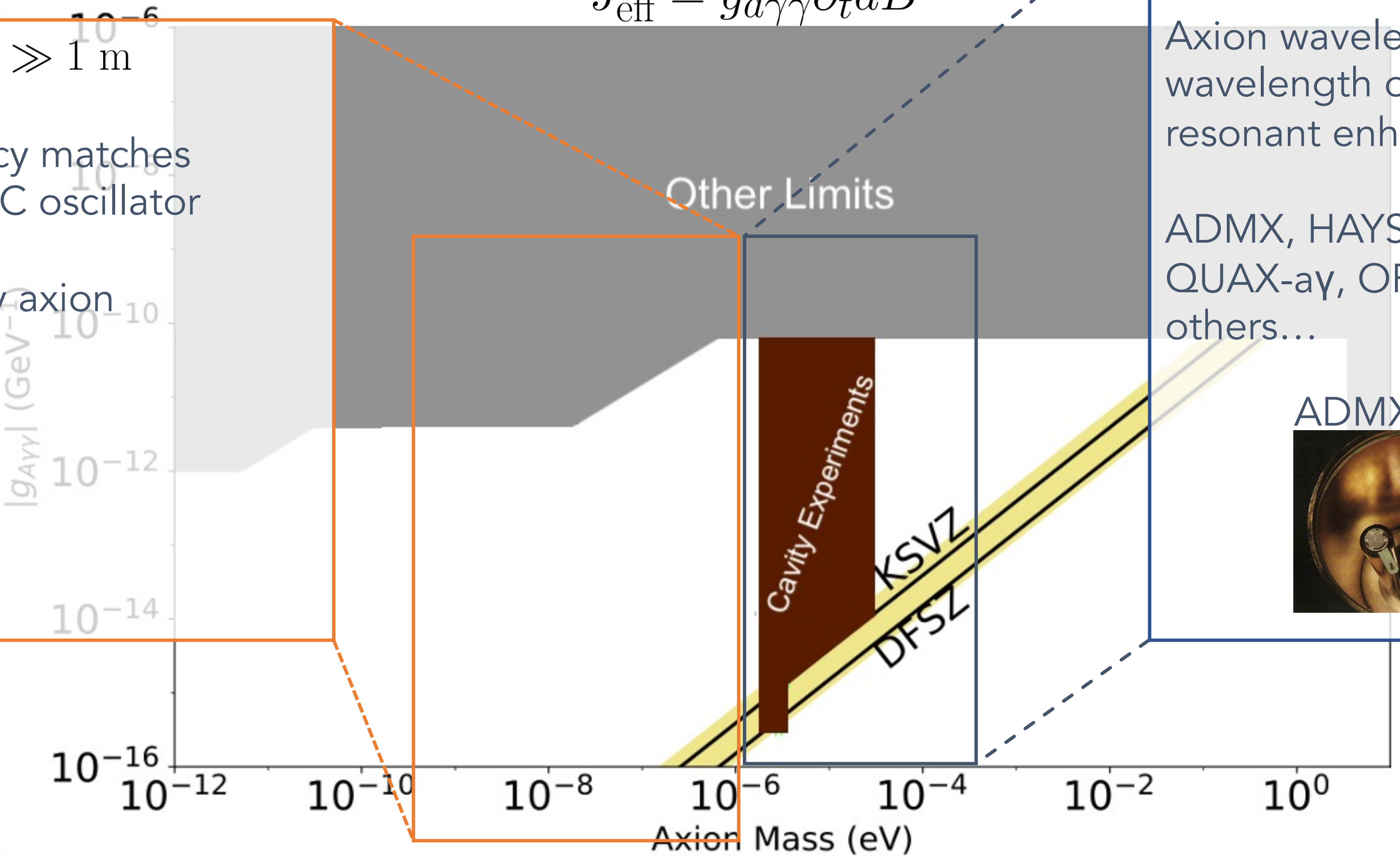

Wavelength $\lambda \lesssim 1\ \text{m}$

Axion wavelength matches wavelength of cavity mode – resonant enhancement

ADMX, HAYSTAC, CAPP-8TB, QUAX-aγ, ORGAN, MADMAX, others…

ADMX

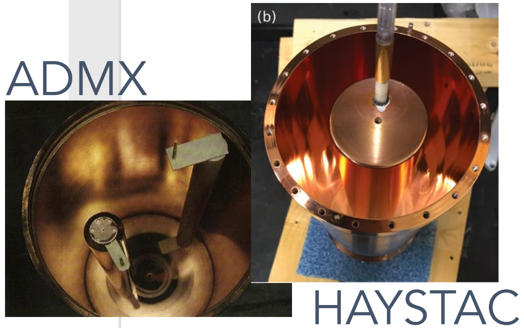

HAYSTAC

Axion Parameter Space

$$\vec{J}_{\text{eff}} = g_{a\gamma\gamma}\partial_t a\vec{B}$$

Wavelength $\lambda \gg 1\ \mathrm{m}$

Axion frequency matches resonance of LC oscillator

Pre-inflationary axion

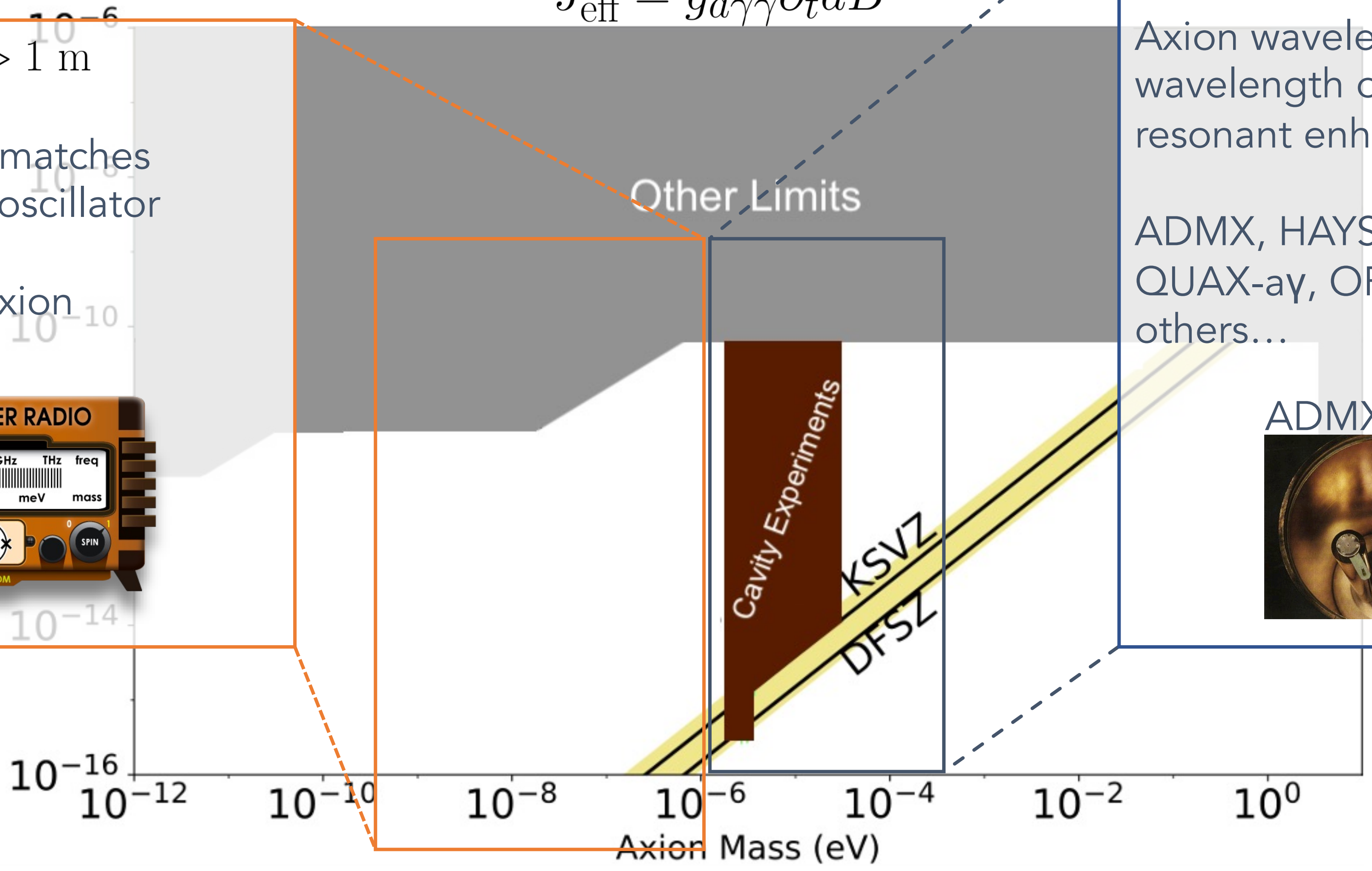

Wavelength $\lambda \lesssim 1\ \mathrm{m}$

Axion wavelength matches wavelength of cavity mode – resonant enhancement

ADMX, HAYSTAC, CAPP-8TB, QUAX-aγ, ORGAN, MADMAX, others…

ADMX

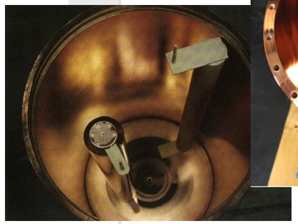

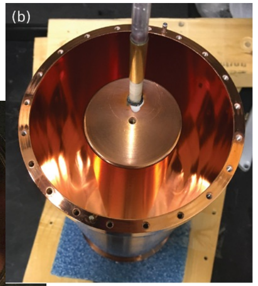

HAYSTAC

Axion Parameter Space

Wavelength $\lambda \gg 1\ \mathrm{m}$

Axion frequency matches resonance of LC oscillator

Pre-inflationary axion

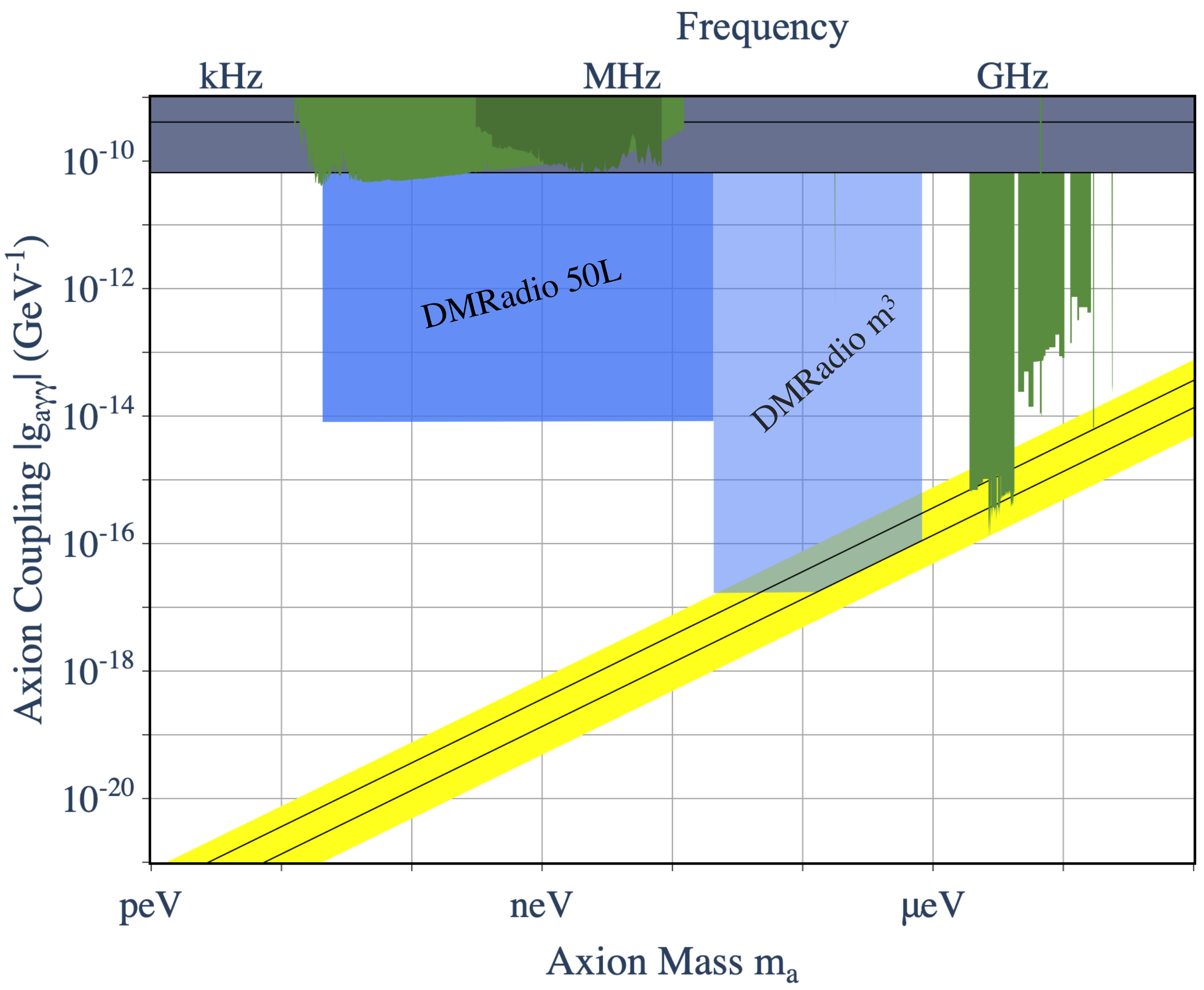

Outline

1. Axions and low frequency haloscopes
2. DMRadio 50L
    1. Overview
    2. Status
3. DMRadio m^3
    1. Overview
    2. Status
4. Outlook, future, & collaboration

50L Goals

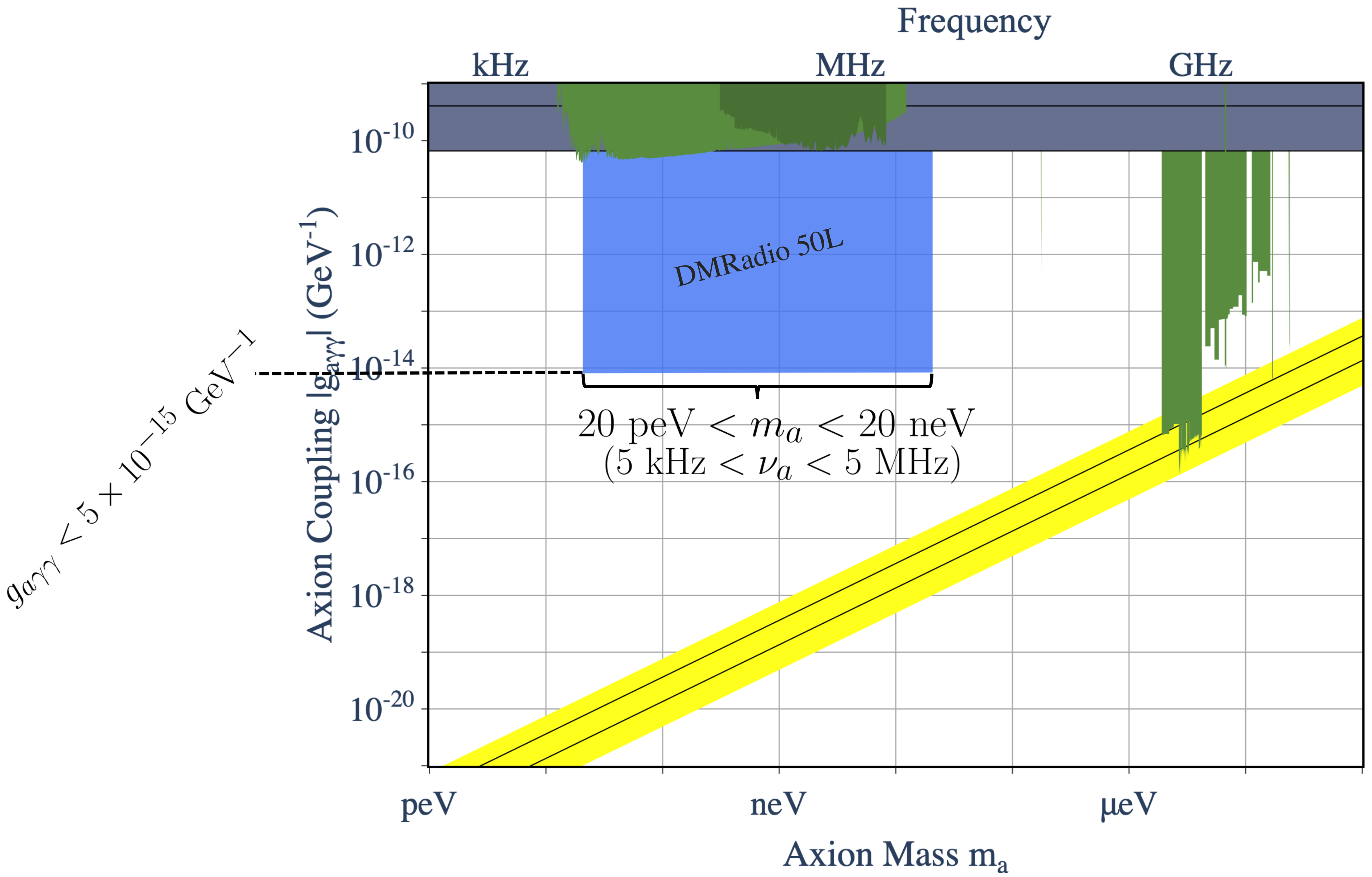

Frequency
kHz
MHz
GHz
DMRadio 50L
20 peV < m_a < 20 neV
(5 kHz < ν_a < 5 MHz)
$g_{a\gamma\gamma} < 5 \times 10^{-15}$ GeV^{-1}
Axion Coupling $|g_{a\gamma\gamma}|$ (GeV^{-1})
10^{-10}
10^{-12}
10^{-14}
10^{-16}
10^{-18}
10^{-20}
peV
neV
μeV
Axion Mass m_a

50L Goals

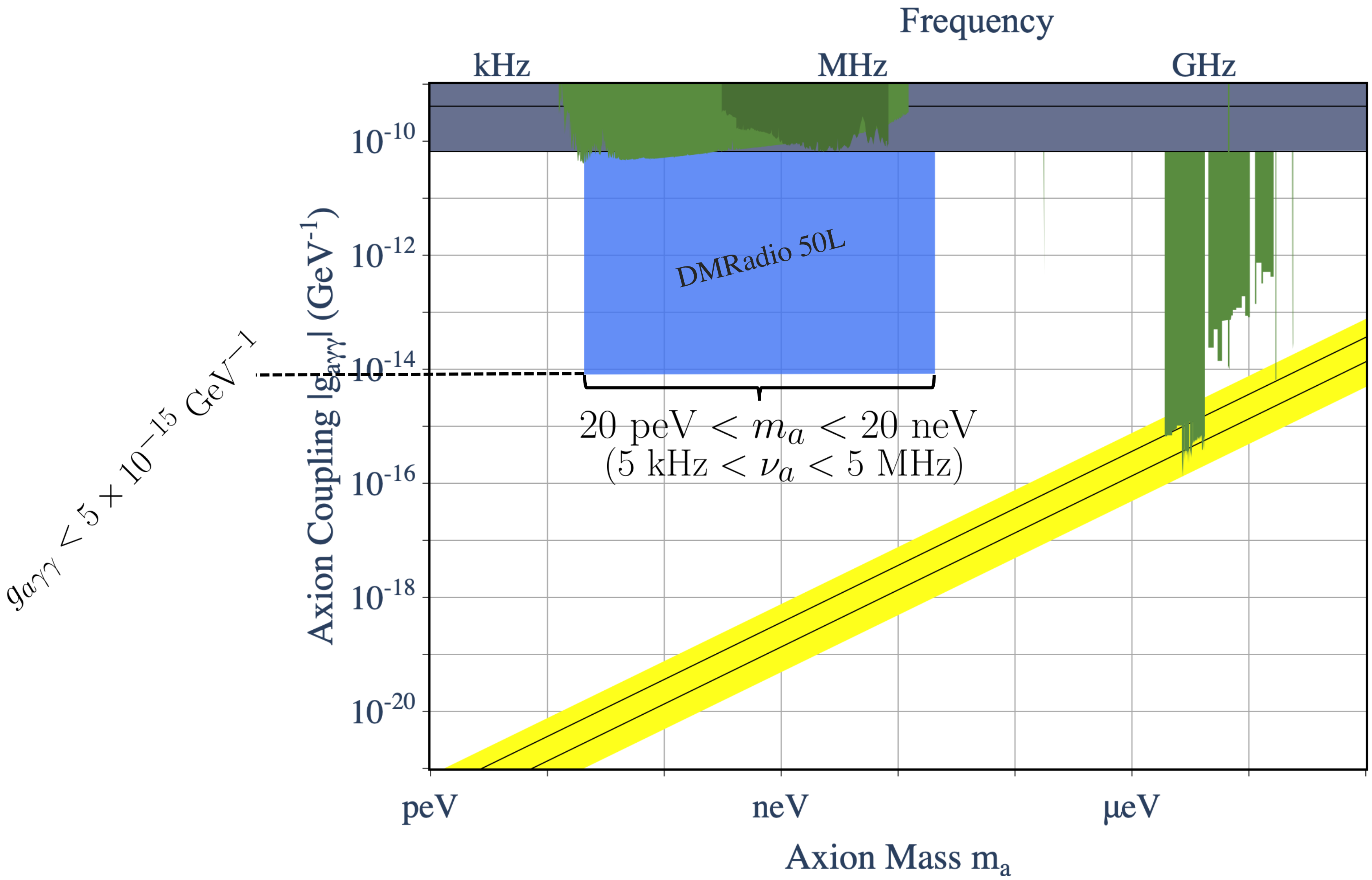

Demonstration of LC resonator + magnet

50L Goals

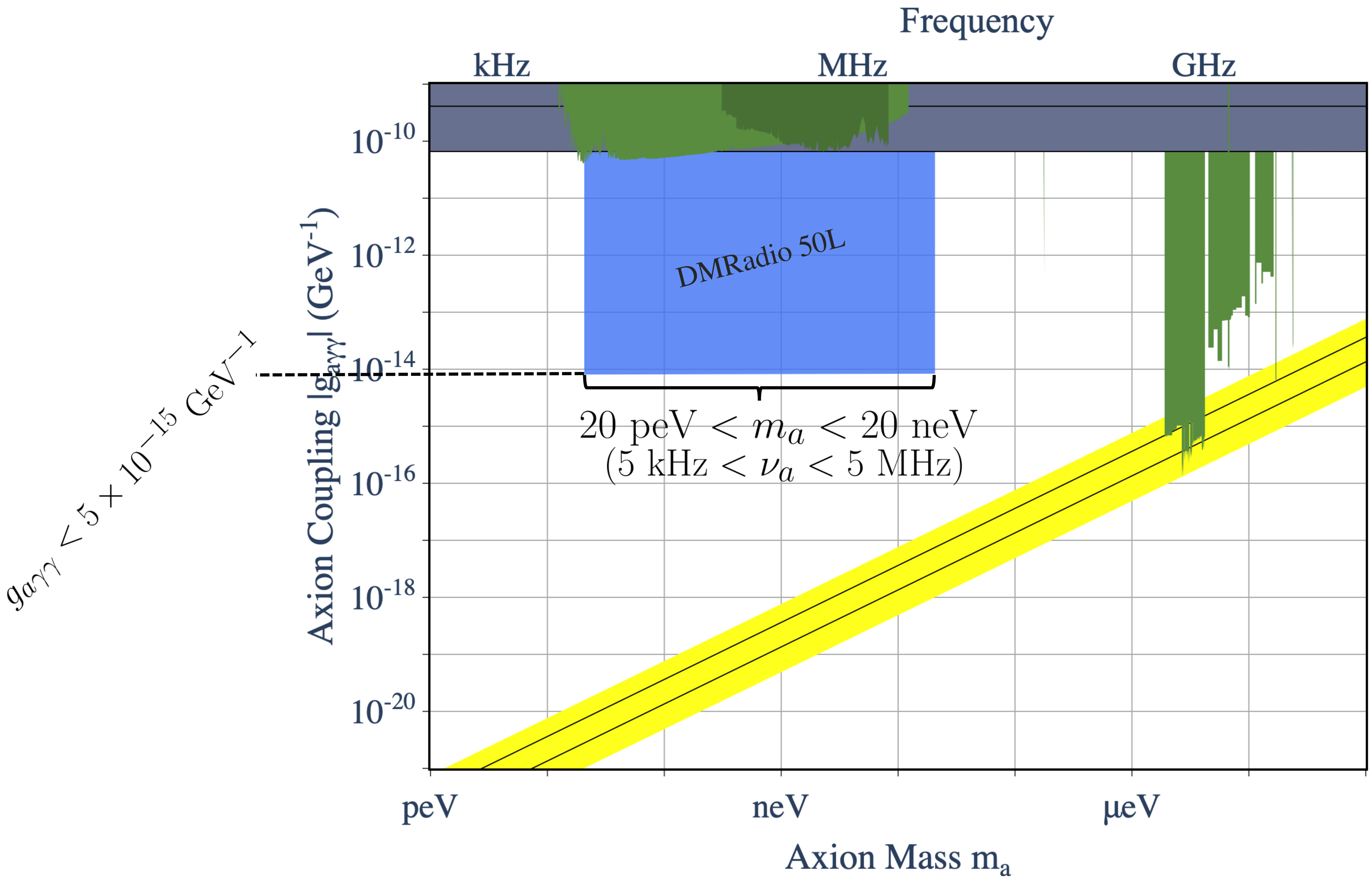

Demonstration of LC resonator + magnet

Testbed for novel quantum devices

50L Circuit & Design

$$\vec{J}_{\rm eff} = g_{a\gamma\gamma}\partial_t a \vec{B}$$

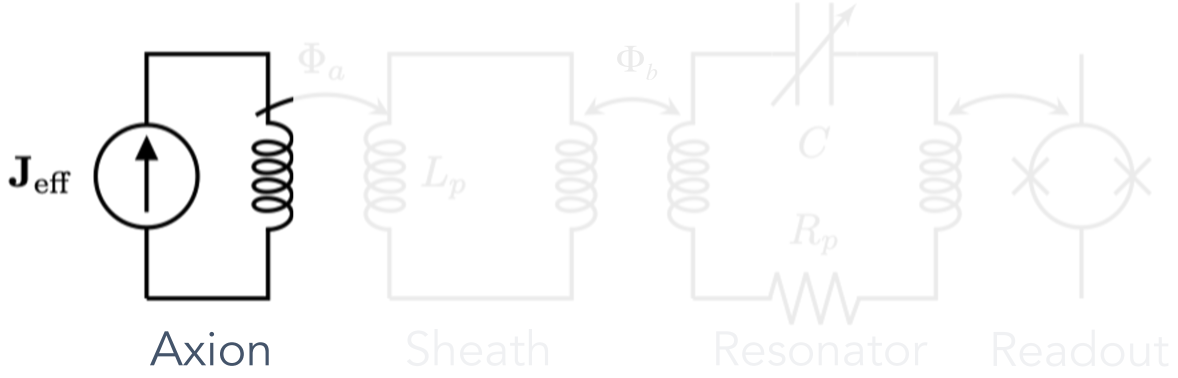

~1 T magnet

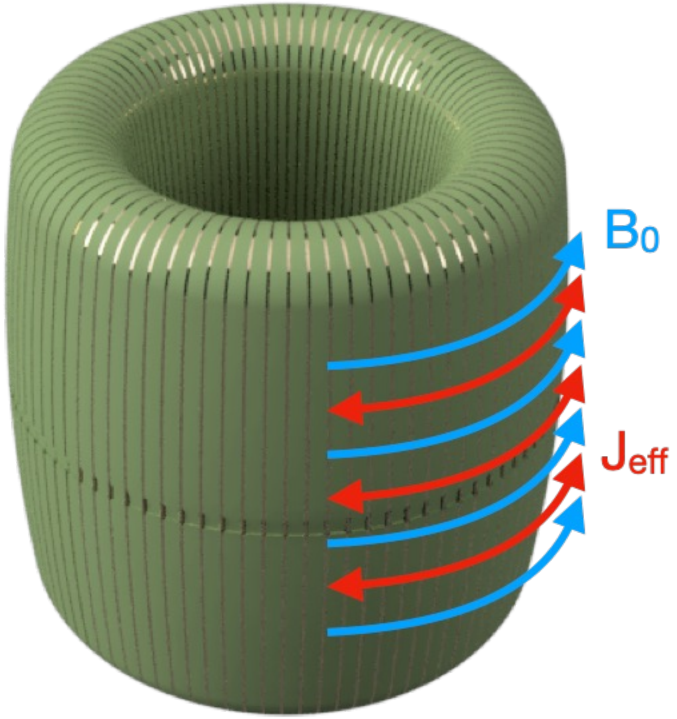

50L Circuit & Design

$$\vec{J}_{\text{eff}} = g_{a\gamma\gamma}\partial_t a\vec{B}$$

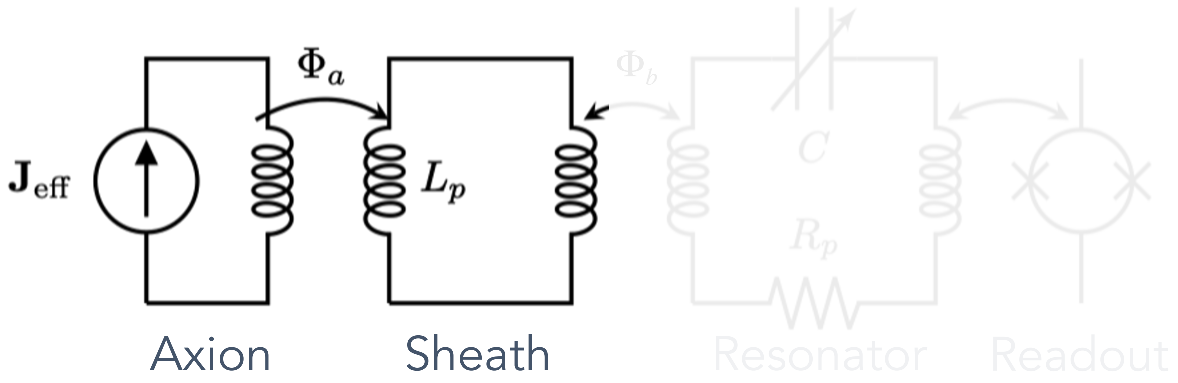

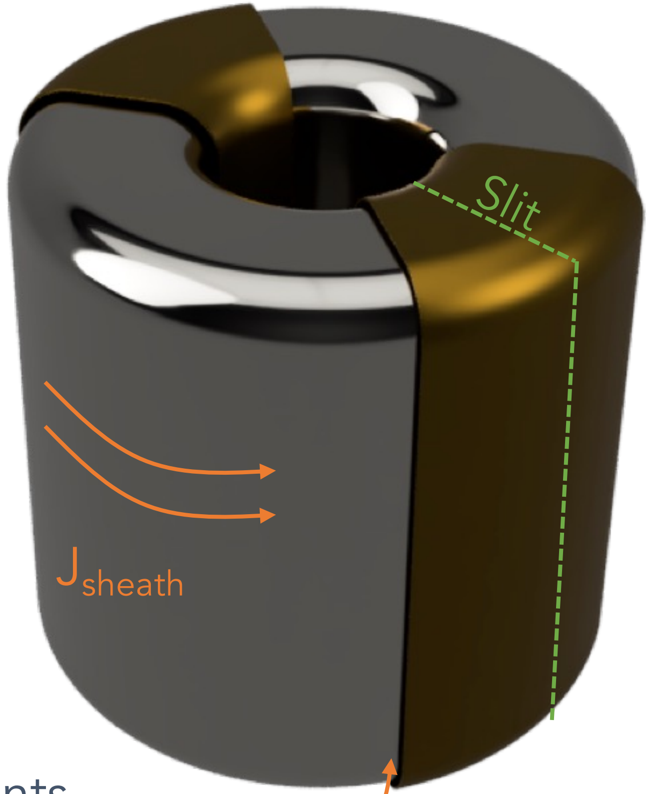

Nb sheath shields lossy magnet elements

Slit (+ sleeve) allows currents to flow outside

50L Circuit & Design

$$\vec{J}_{\text{eff}} = g_{a\gamma\gamma}\partial_t a\vec{B}$$

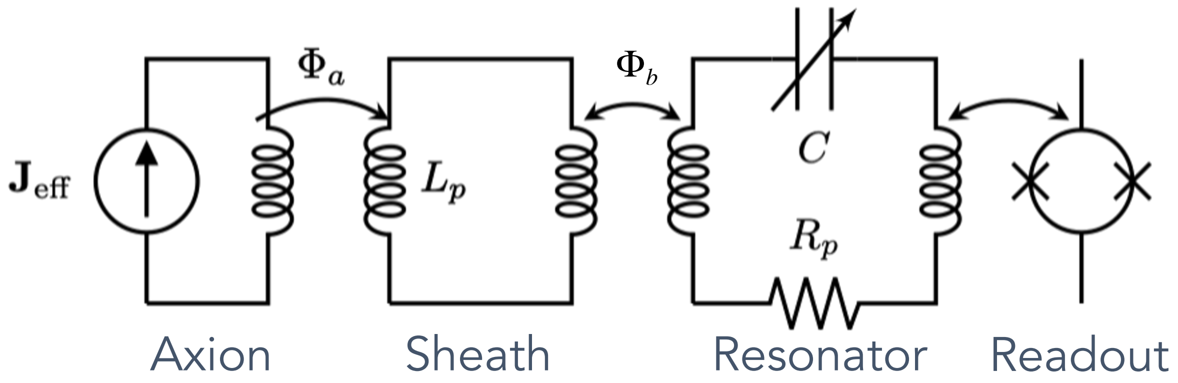

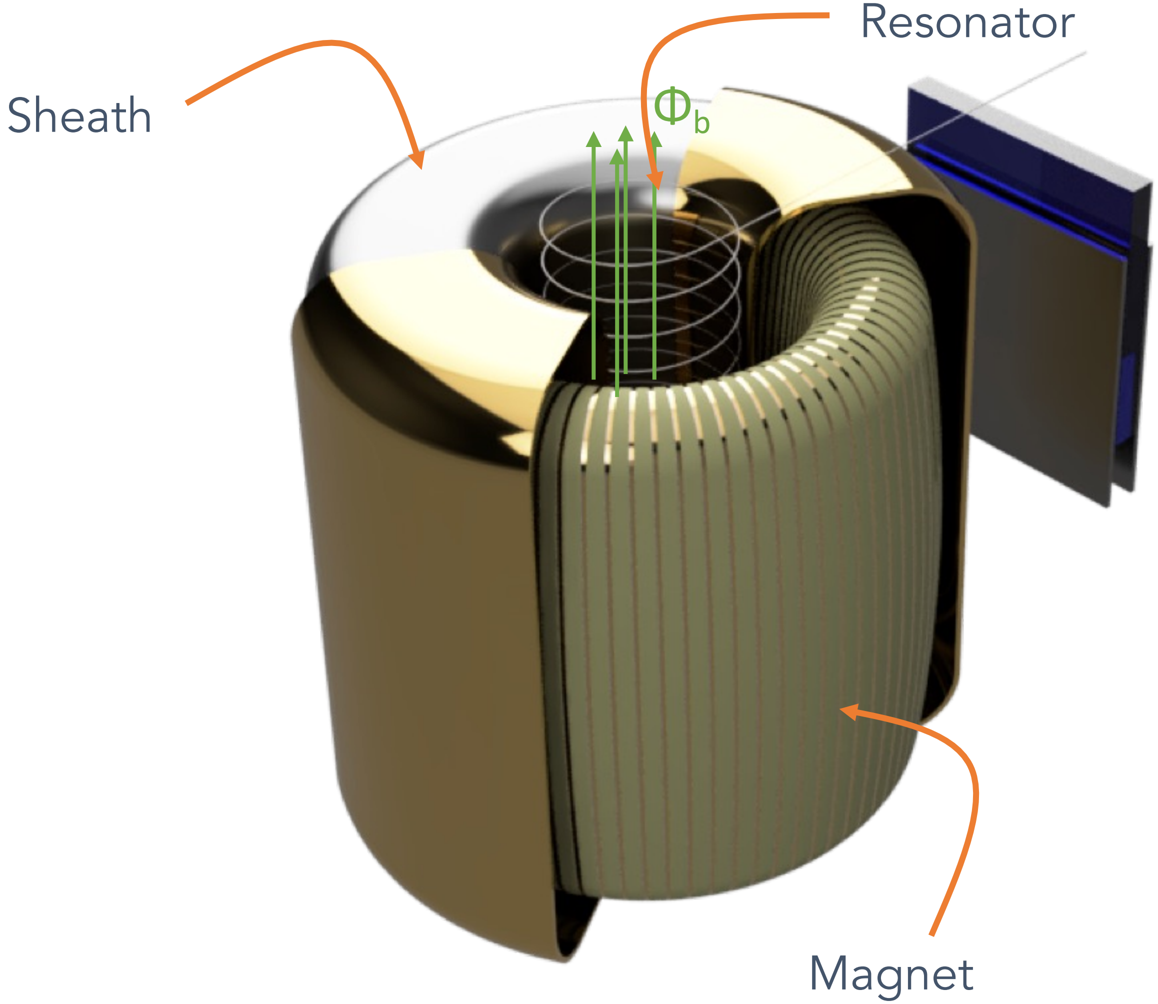

50L Circuit & Design

$$\vec{J}_{\text{eff}} = g_{a\gamma\gamma}\partial_t a\vec{B}$$

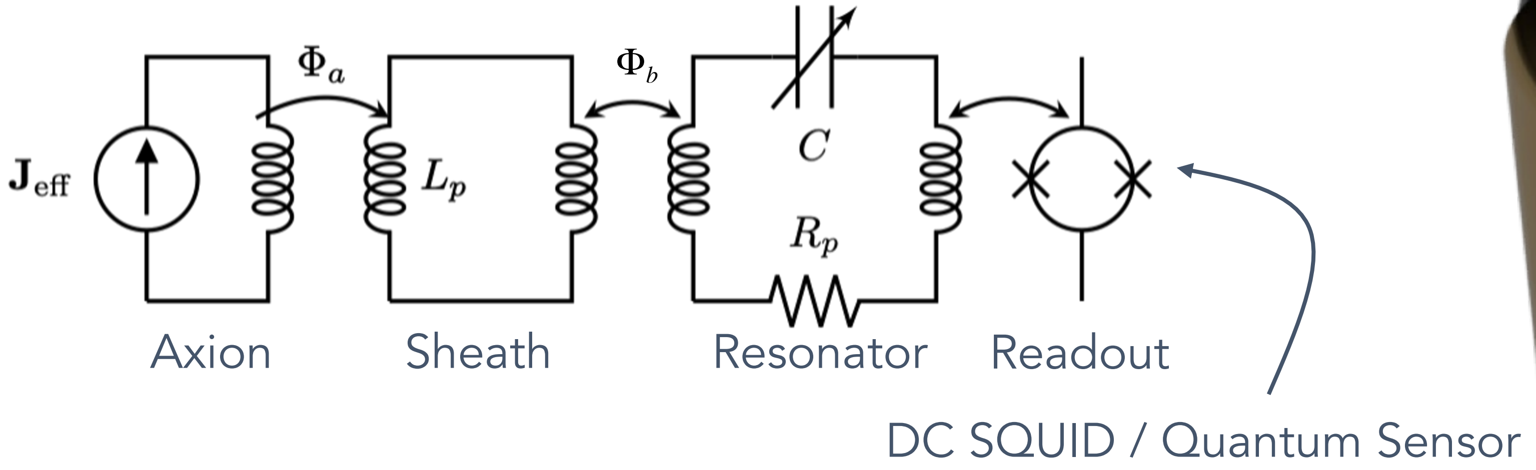

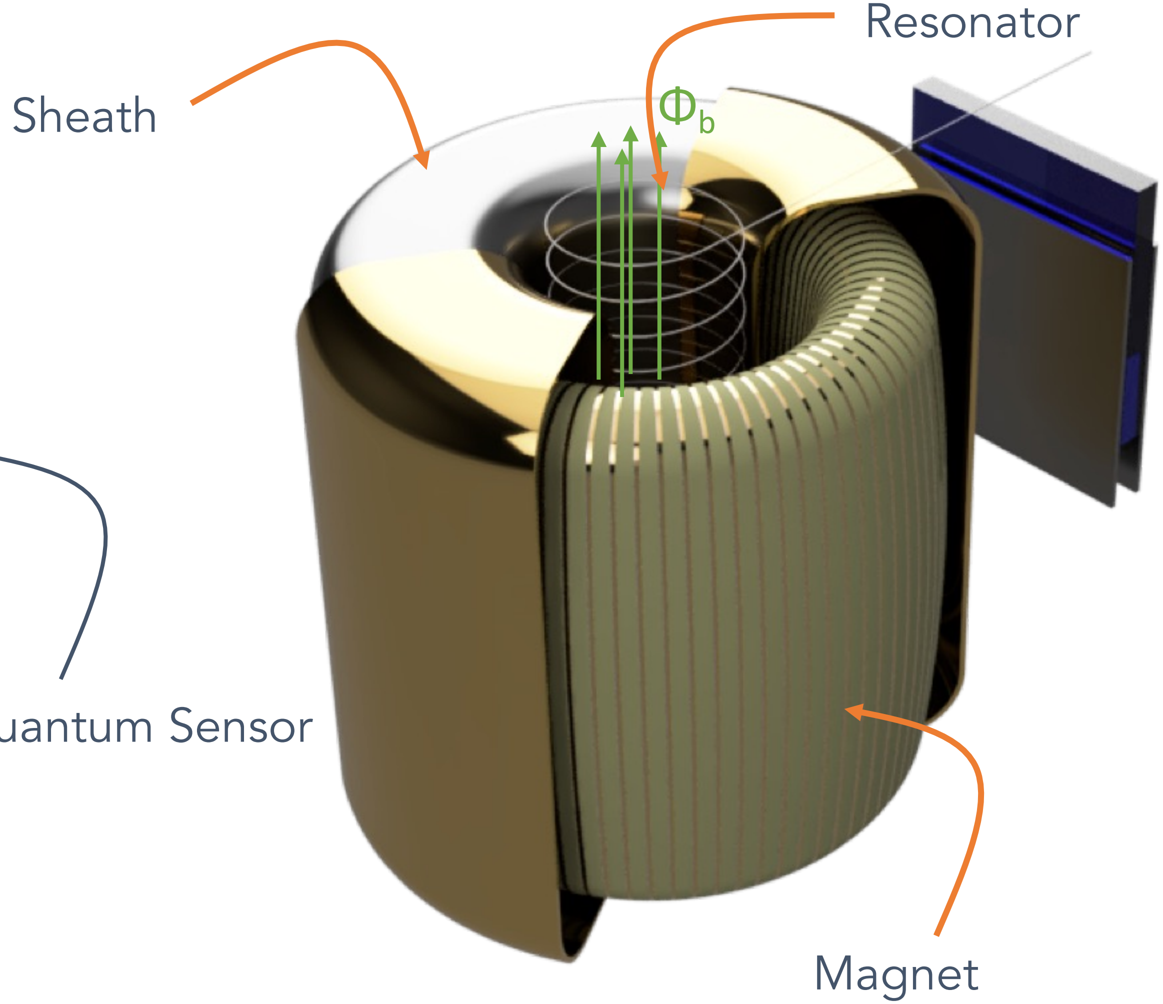

50L Circuit & Design

$$\vec{J}_{\text{eff}} = g_{a\gamma\gamma}\partial_t a\vec{B}$$

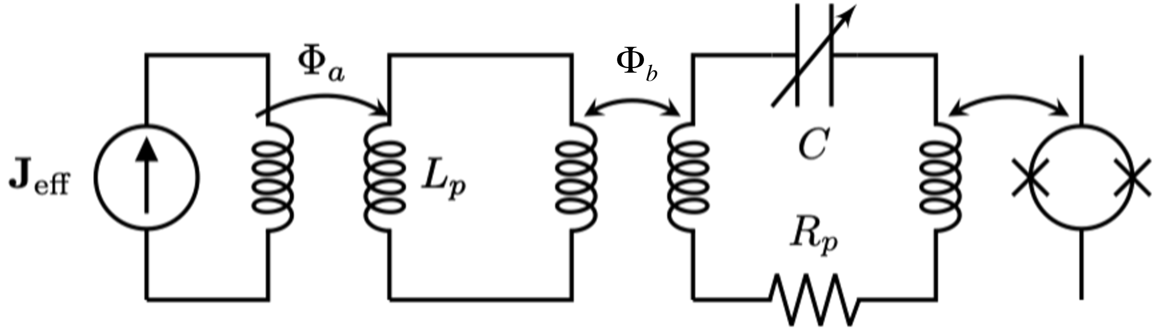

DC SQUID / Quantum Sensor

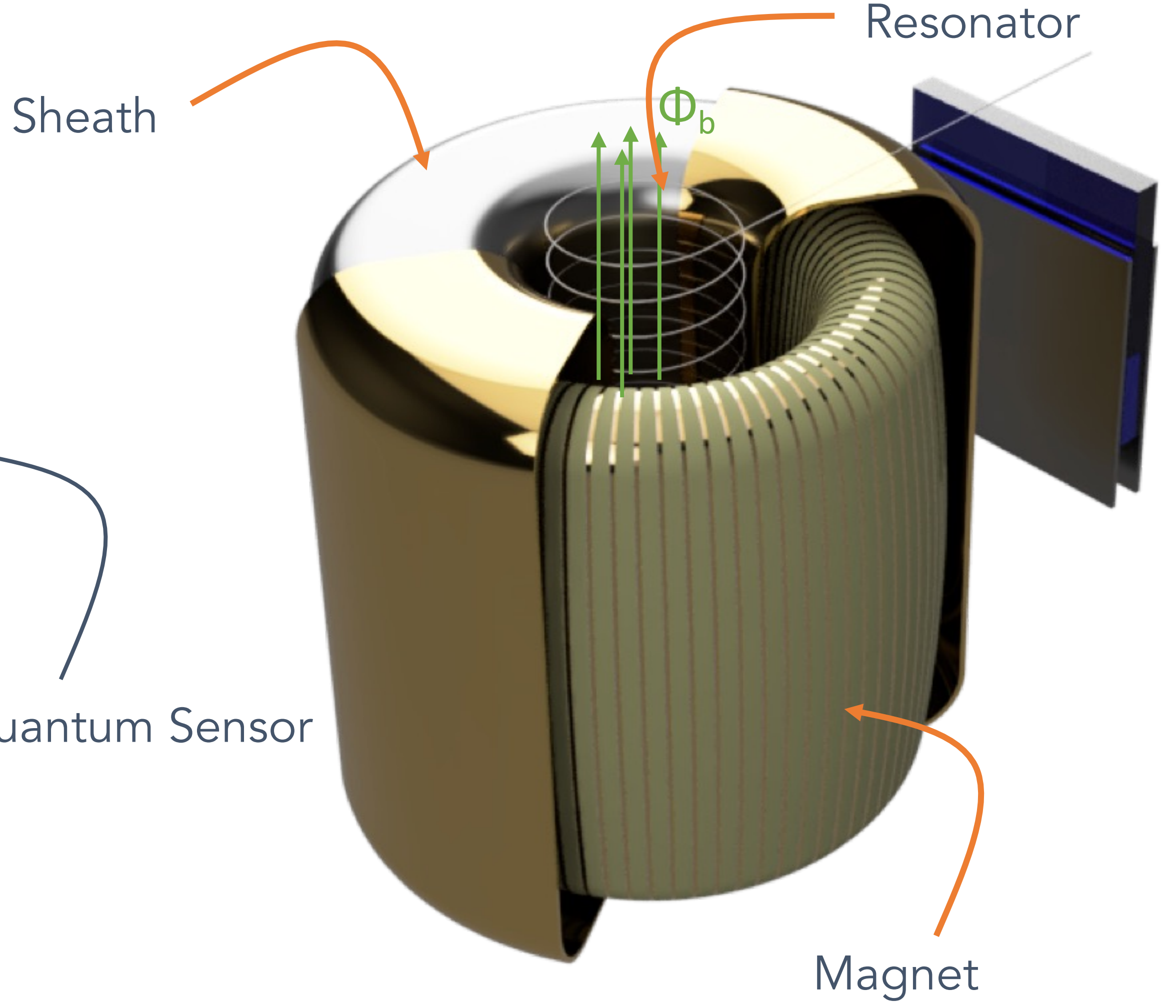

Quality factor of circuit ~10^6

Peak B-field ~ 1 T

Physical temperature of resonator < 100 mK

Built at Stanford University

Integrated Sensitivity and Quantum Sensors

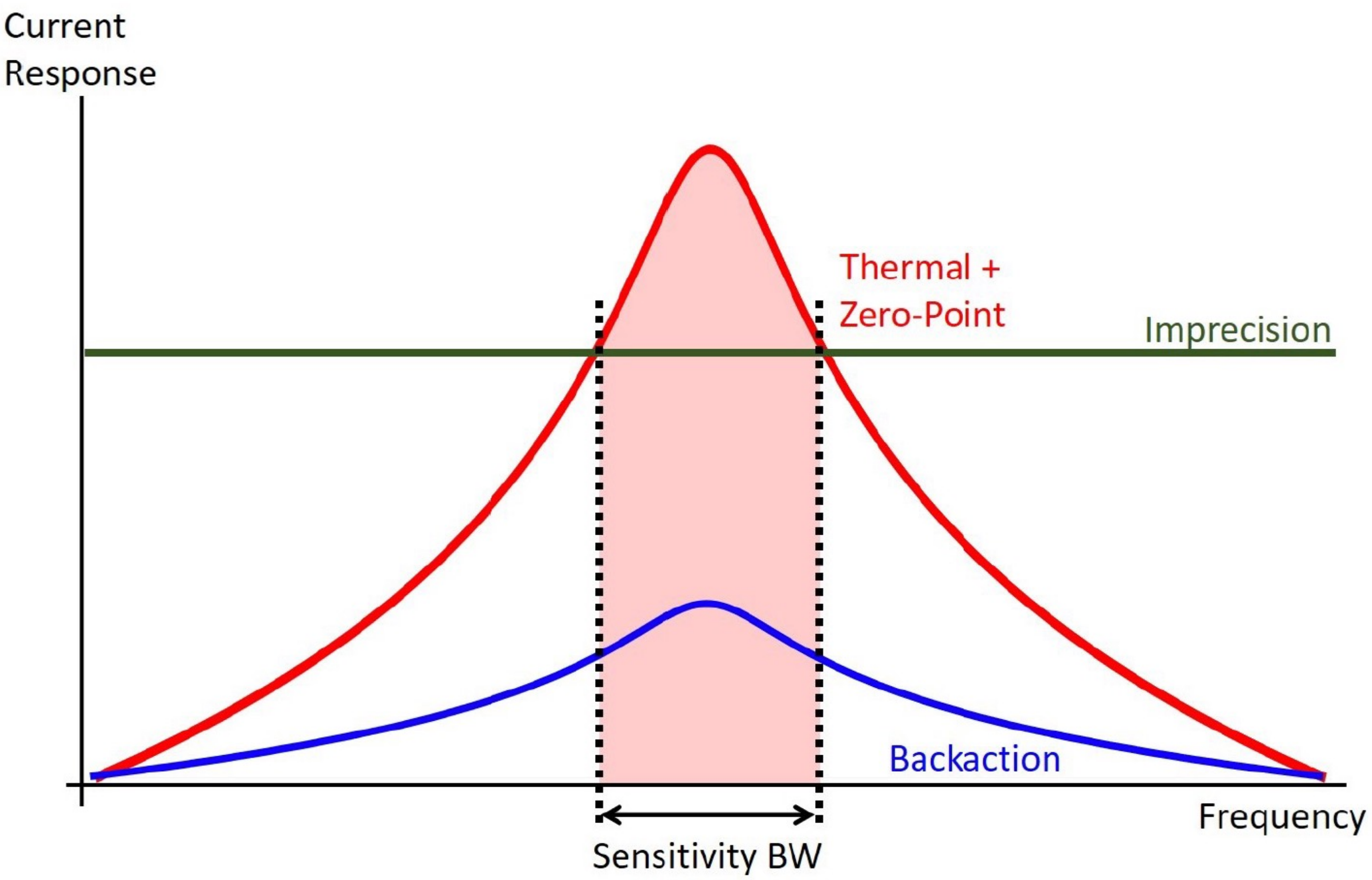

Integrated Sensitivity and Quantum Sensors

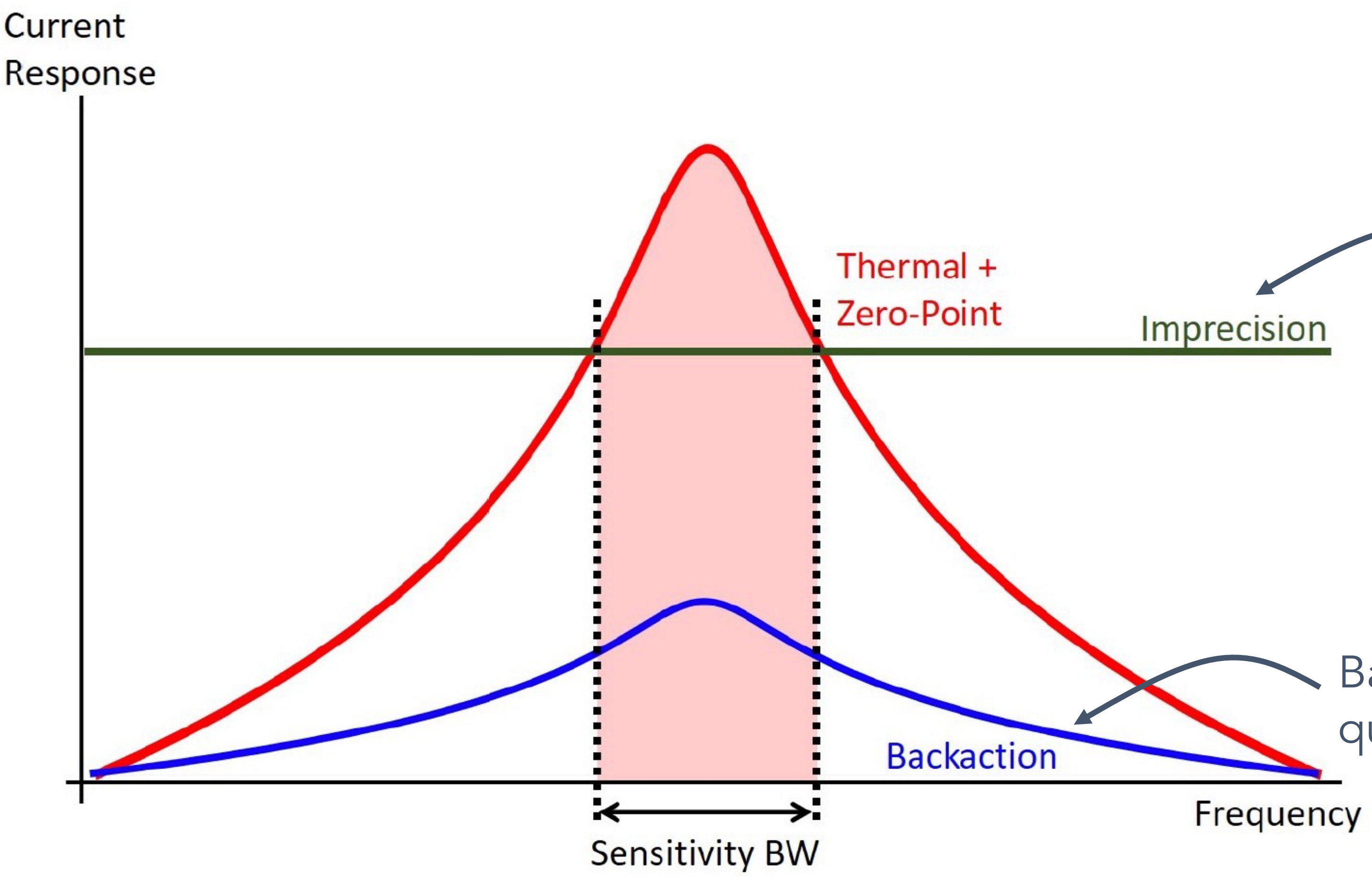

Uncertainty in measurement

Backaction due to process of quantum measurement of state

Integrated Sensitivity and Quantum Sensors

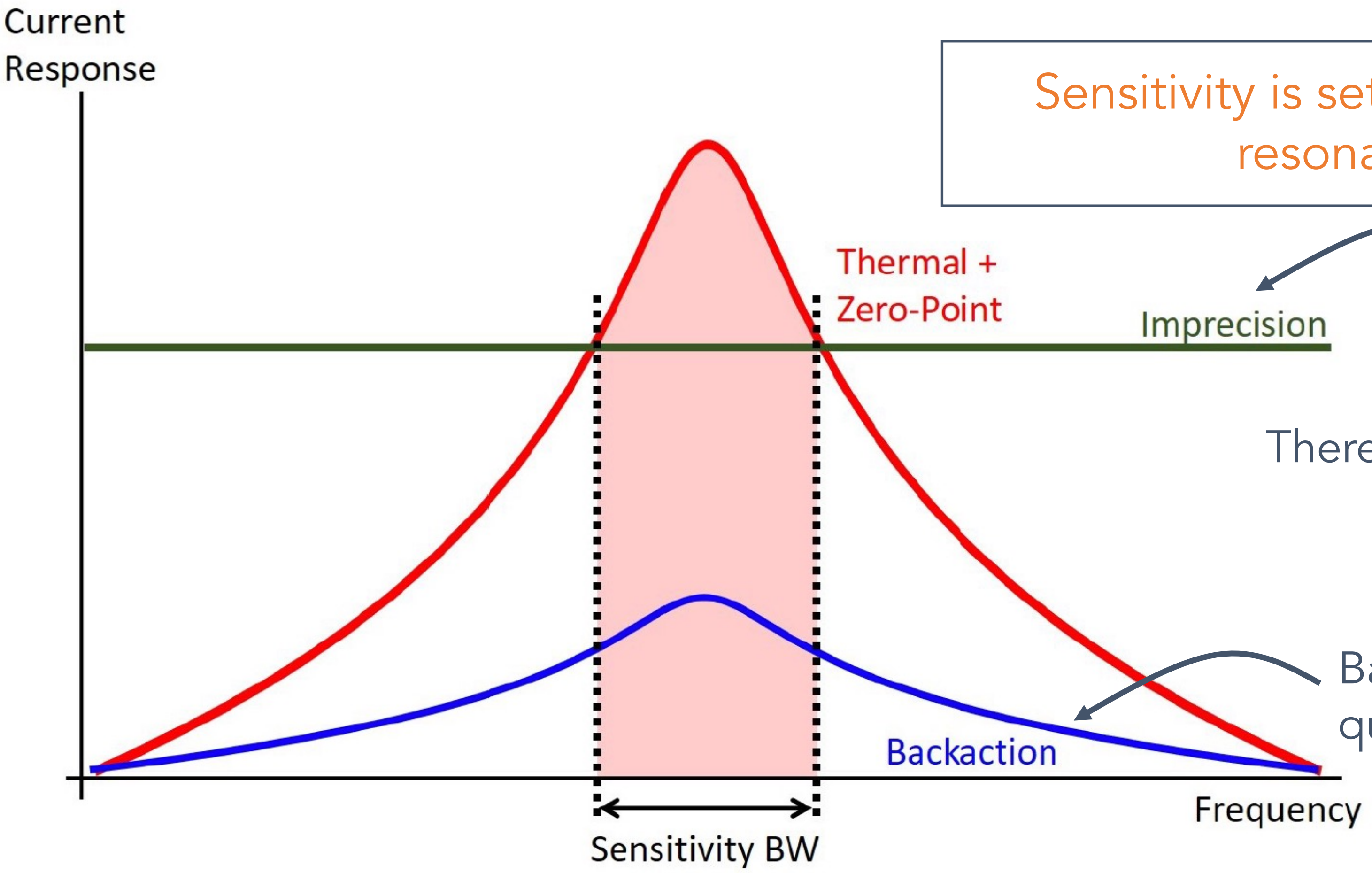

Sensitivity is set by bandwidth, not on resonance behavior

Uncertainty in measurement

There exists a tradeoff between backaction and imprecision noise

Backaction due to process of quantum measurement of state

Integrated Sensitivity and Quantum Sensors

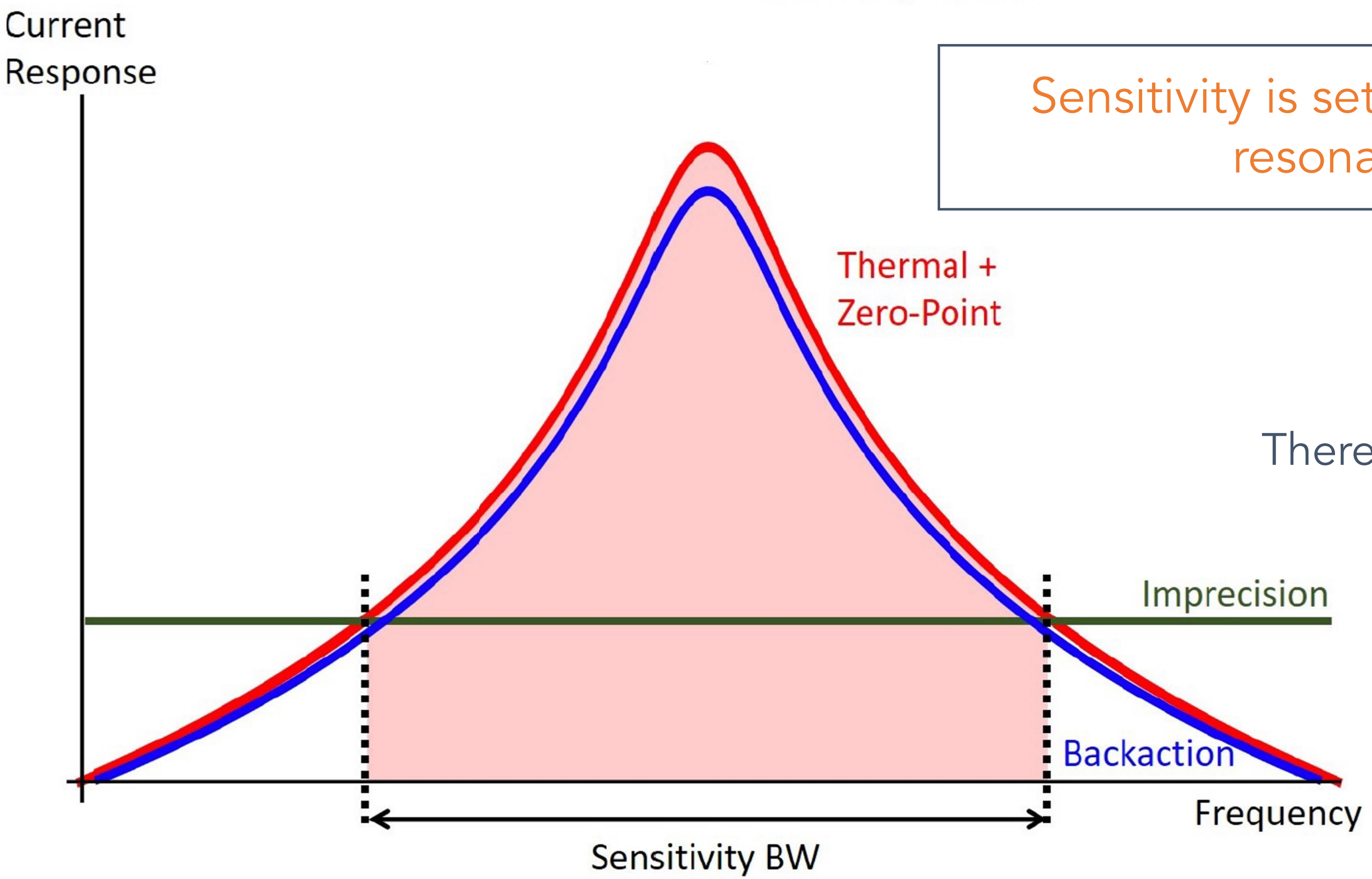

Sensitivity is set by bandwidth, not on resonance behavior

There exists a tradeoff between backaction and imprecision noise

50L Status

BlueFors Dil Fridge at Stanford

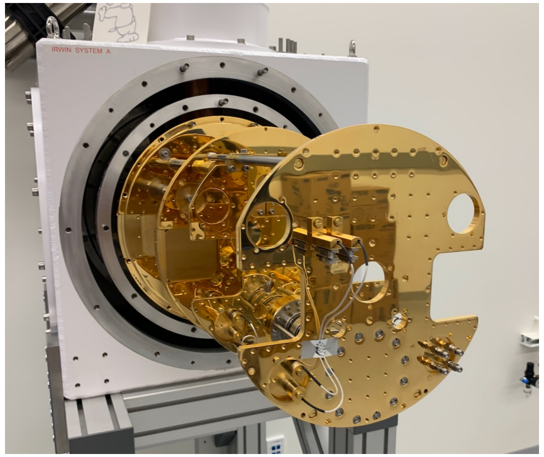

50L Status

BlueFors Dil Fridge at Stanford

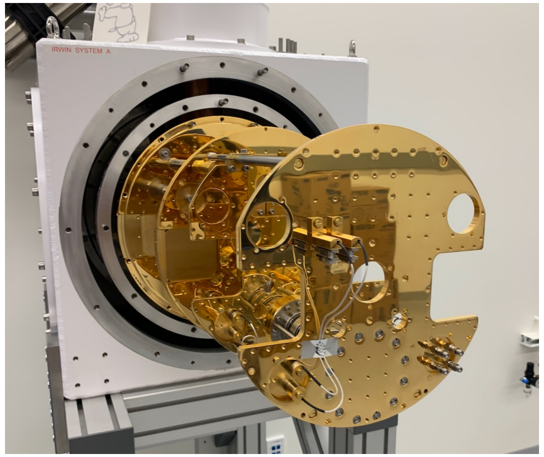

Cryostat currently being manufactured

50L Status

BlueFors Dil Fridge at Stanford

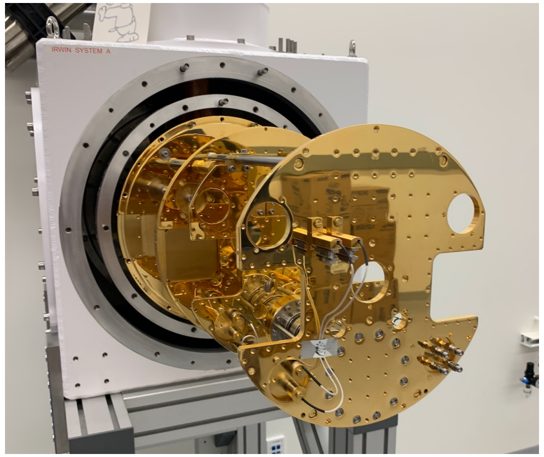

Cryostat currently being manufactured

Magnet being manufactured by SSI

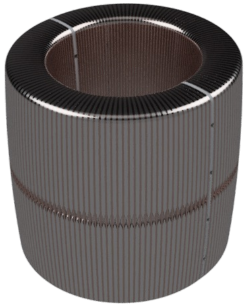

50L Status

BlueFors Dil Fridge at Stanford

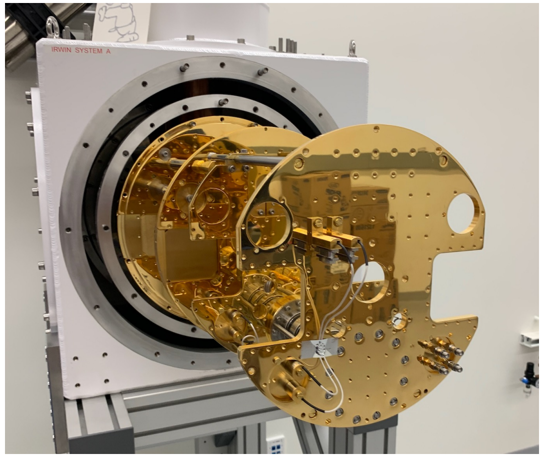

Cryostat currently being manufactured

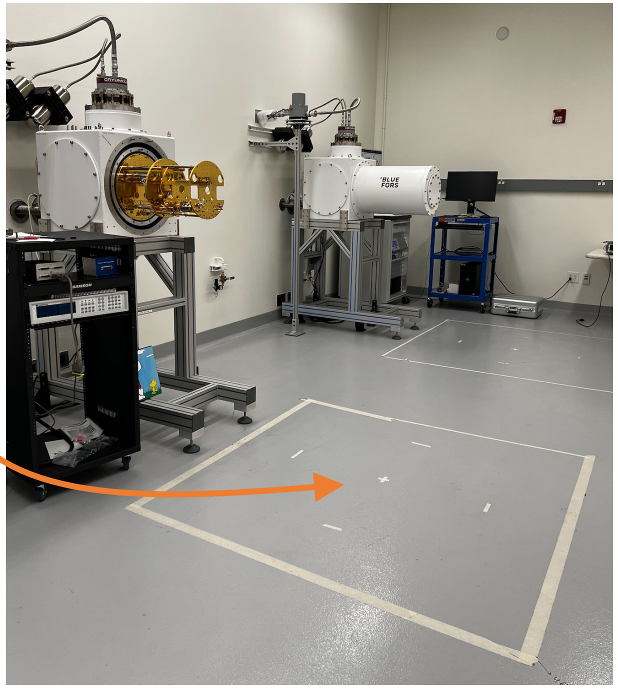

Magnet being manufactured by SSI

Sheath design being finalized

50L Status

BlueFors Dil Fridge at Stanford

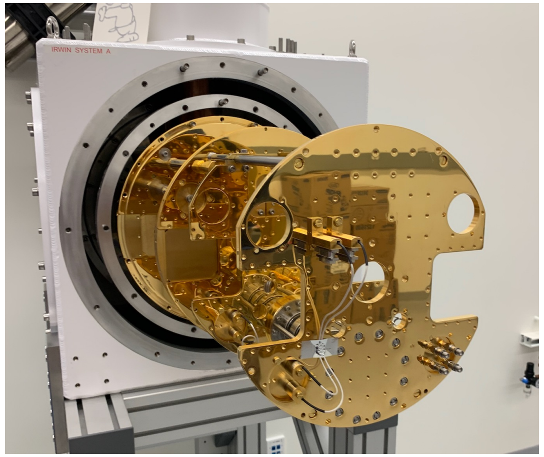

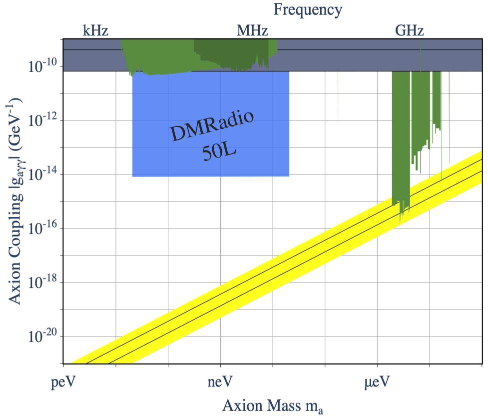

Cryostat currently being manufactured

Science starting in 2023

Magnet being manufactured by SSI

Sheath design being finalized

Outline

1. Axions and low frequency haloscopes
2. DMRadio 50L
    1. Overview
    2. Status
3. DMRadio m^3
    1. Overview
    2. Status
4. Outlook, future, & collaboration

DMRadio m^3 Goals

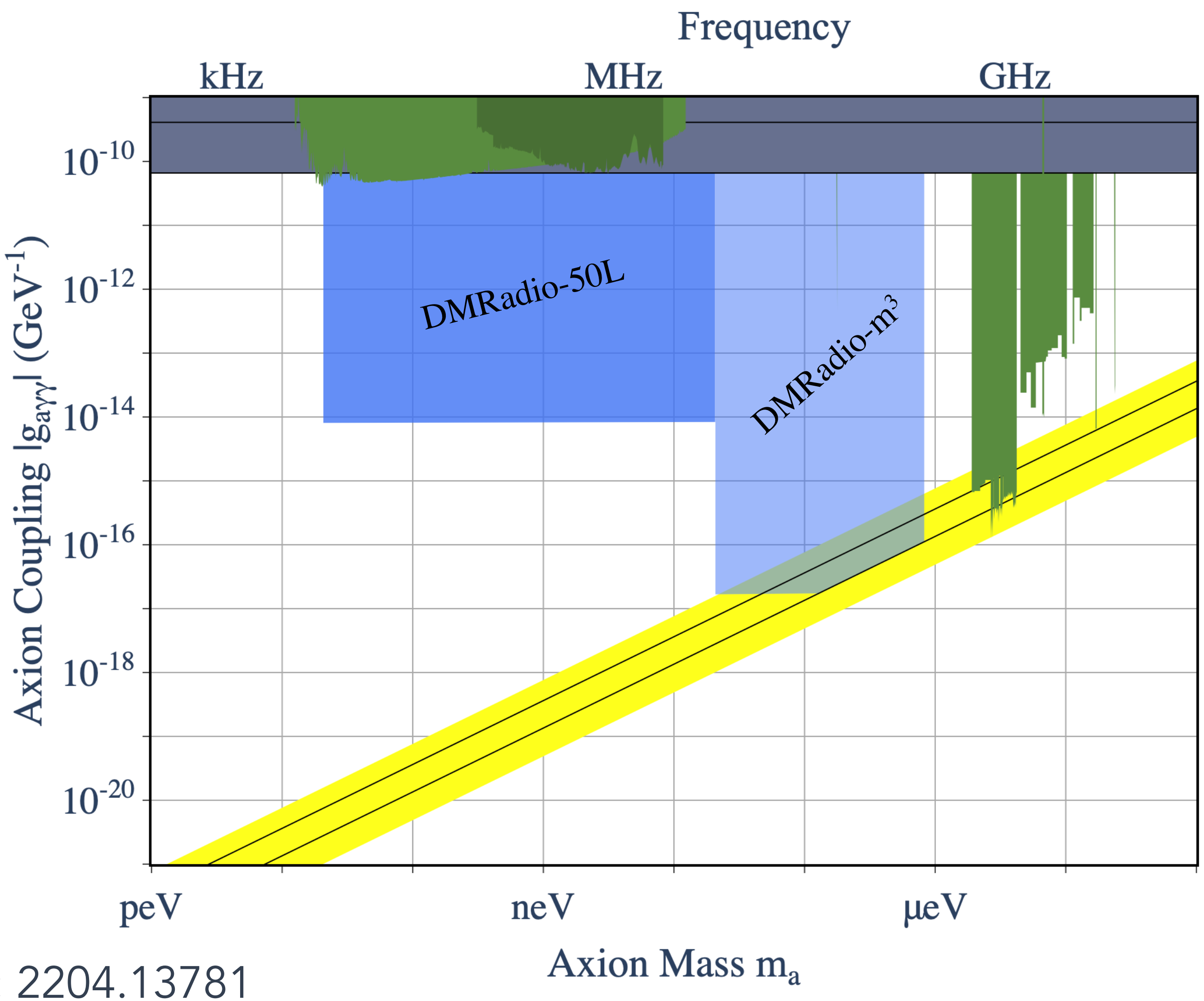

arXiv: 2204.13781

DMRadio m^3 Goals

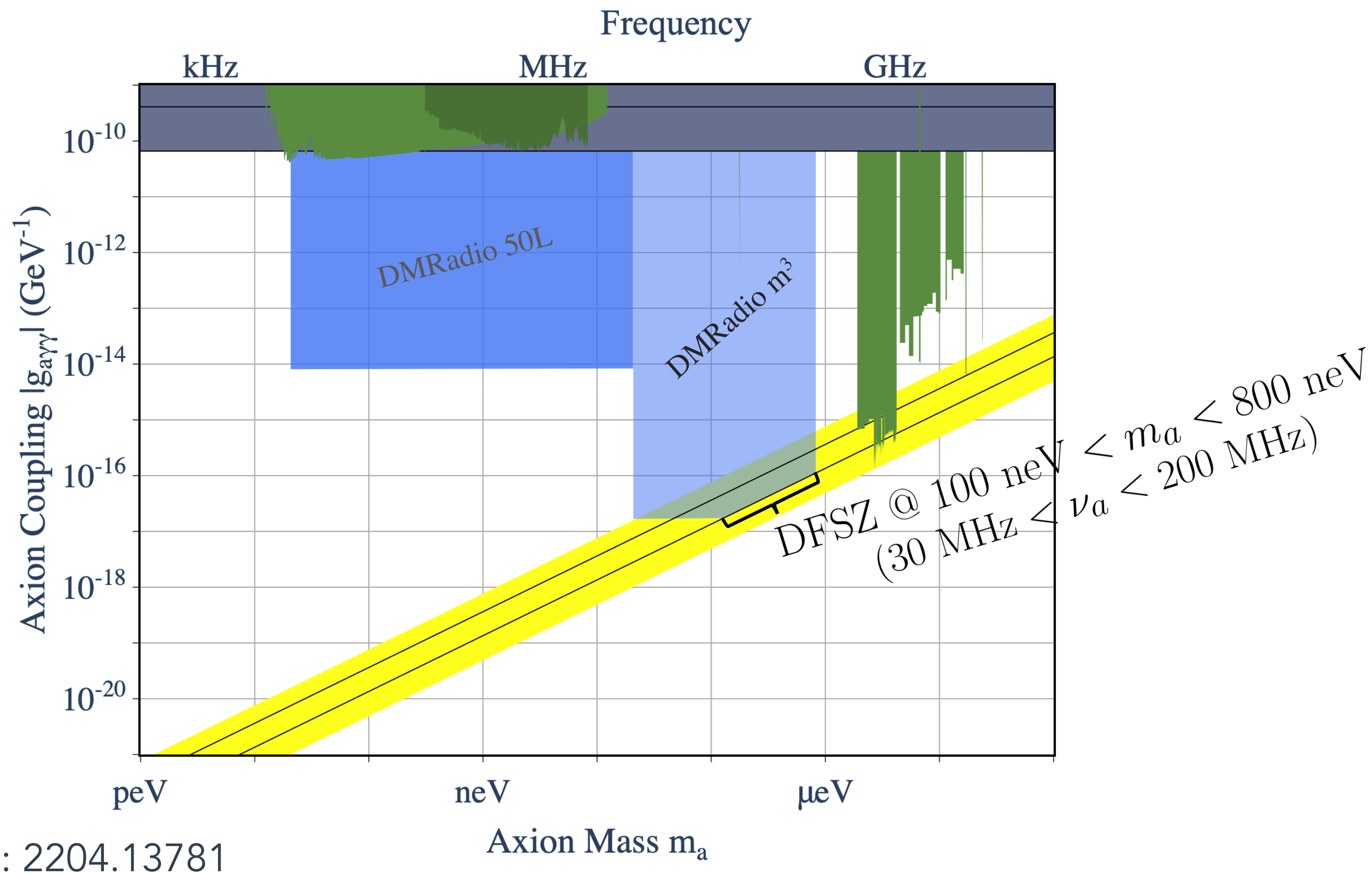

arXiv: 2204.13781

DMRadio m^3 Goals

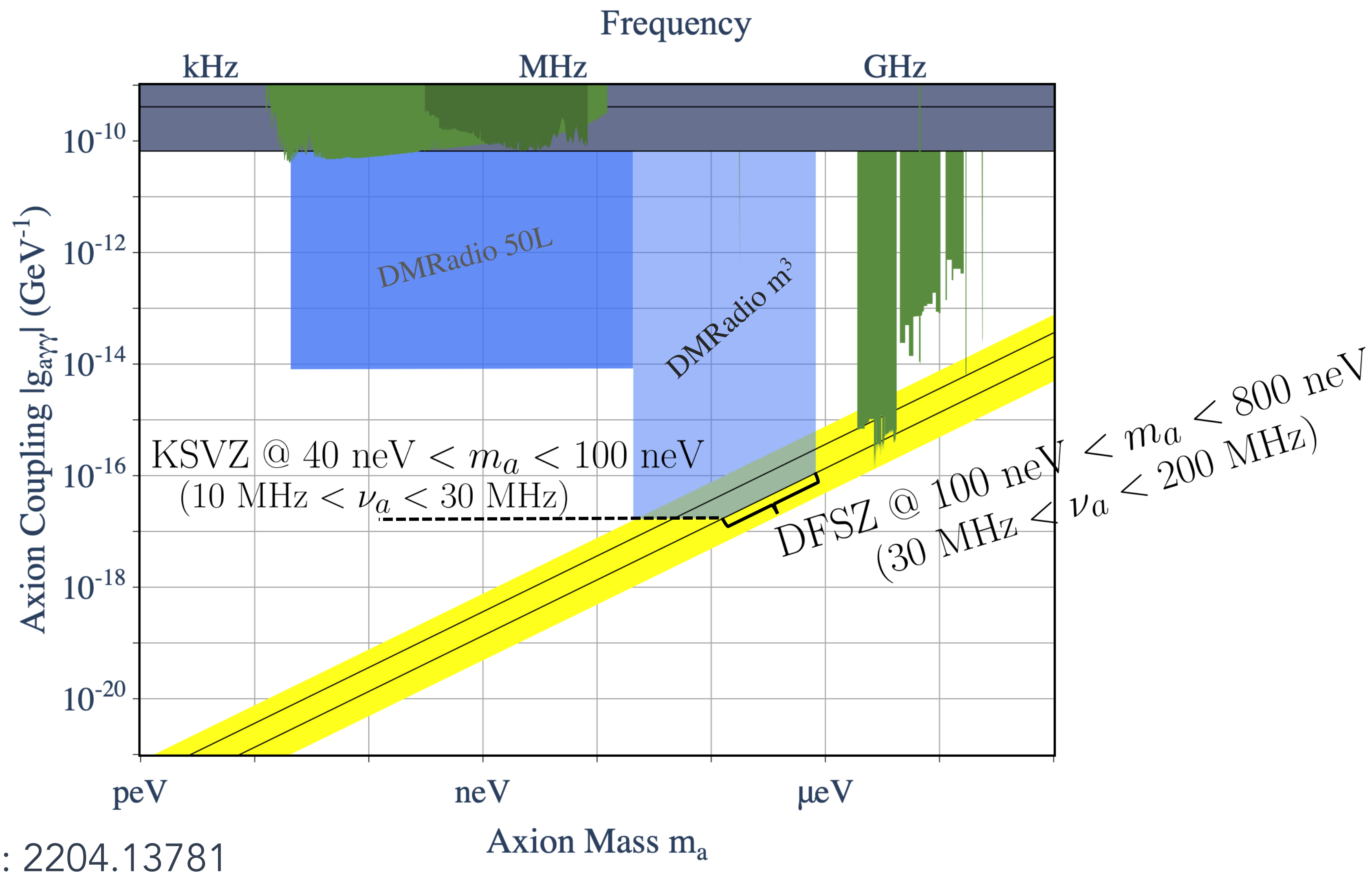

arXiv: 2204.13781

DMRadio m^3 Goals

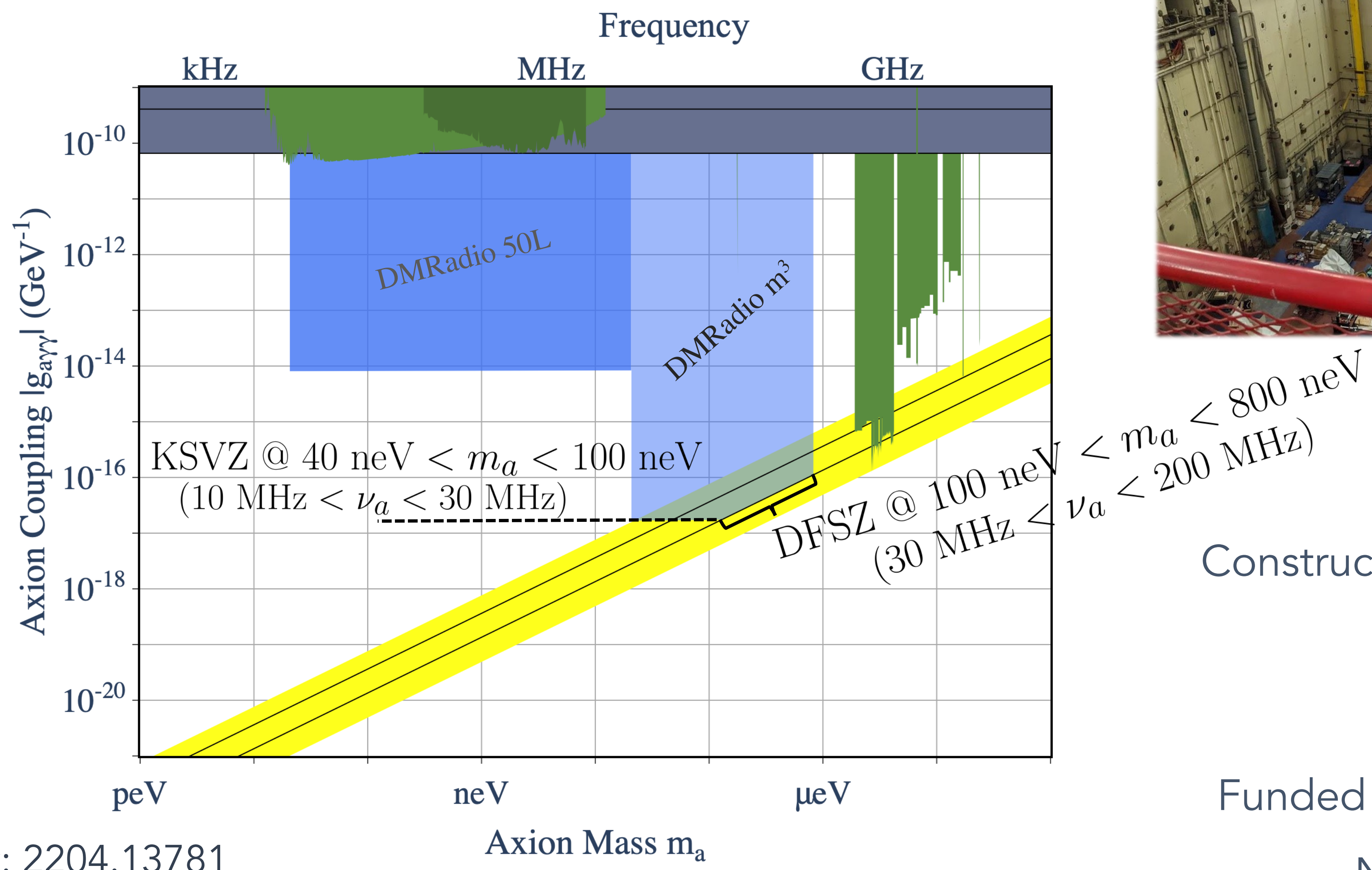

arXiv: 2204.13781

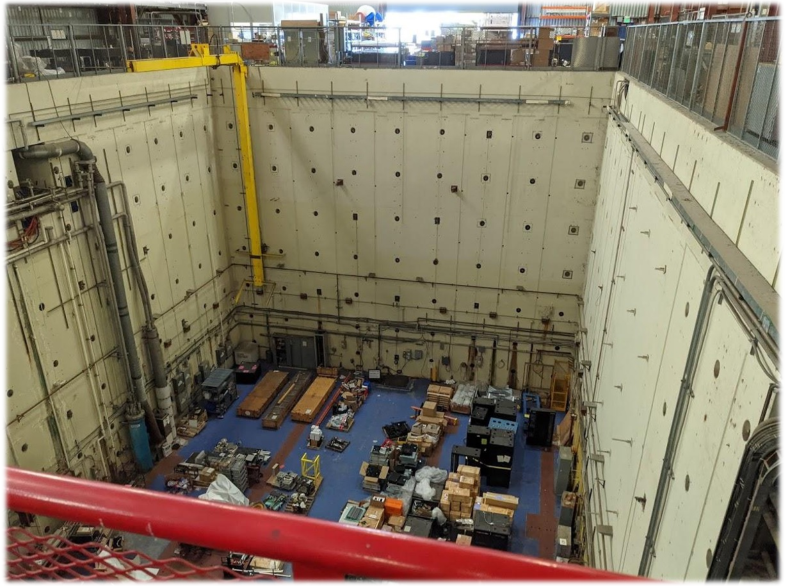

Construction at SLAC National Laboratory

Funded by DOE Dark Matter New Initiatives

DMRadio m^3 Design

50L-like geometry non optimal – problems at high frequency

DMRadio m^3 Design

Parasitic capacitive coupling shorts out signal!

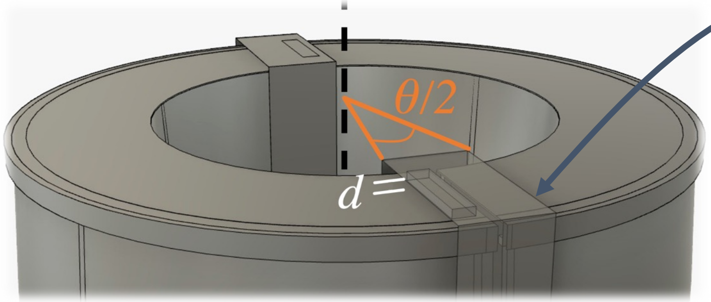

DMRadio 50L

50L-like geometry non optimal – problems at high frequency

DMRadio m^3 Design

Parasitic capacitive coupling shorts out signal!

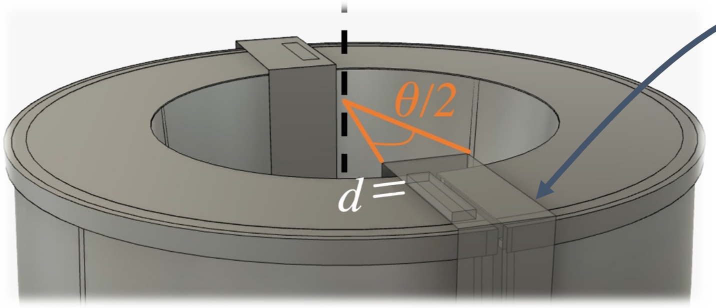

DMRadio 50L

$$f_{\text{paras}} = 48.5\ \text{MHz} \left(\frac{0.05\ \text{m}^3}{V_{\text{sheath}}}\right)^{1/2} \left(\frac{1\ \text{rad}}{\theta}\right)^{1/2} \left(\frac{d}{1\ \text{cm}}\right)^{1/2}$$

50L-like geometry non optimal – problems at high frequency

DMRadio m^3 Design

Parasitic capacitive coupling shorts out signal!

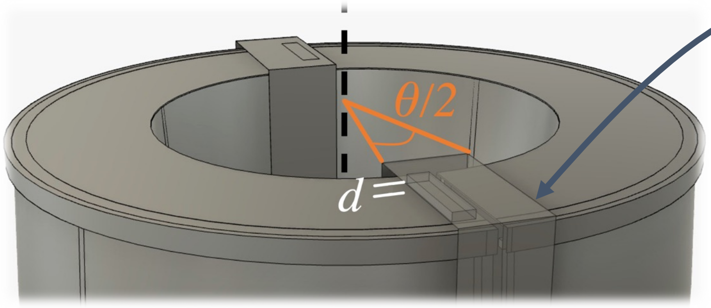

DMRadio 50L

$$f_{\text{paras}} = 48.5\ \text{MHz} \left(\frac{0.05\ \text{m}^3}{V_{\text{sheath}}}\right)^{1/2} \left(\frac{1\ \text{rad}}{\theta}\right)^{1/2} \left(\frac{d}{1\ \text{cm}}\right)^{1/2}$$

50L-like geometry non optimal – problems at high frequency

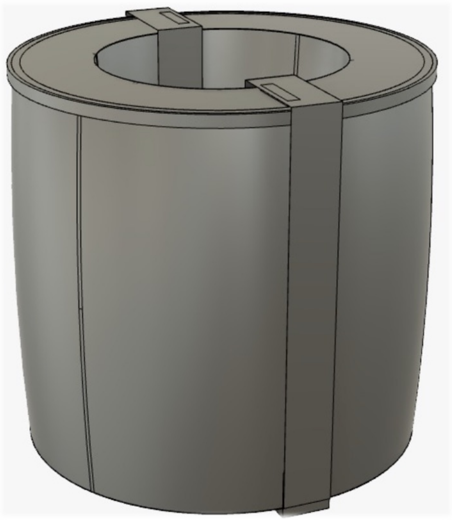

Axion signal will destructively interfere with **cavity modes** of this coaxial structure (as $\lambda \sim l$)

m^3 design

m^3 uses a solenoidal magnet + coaxial copper pickup

No parasitic capacitance

m^3 design

m^3 uses a solenoidal magnet + coaxial copper pickup

No parasitic capacitance

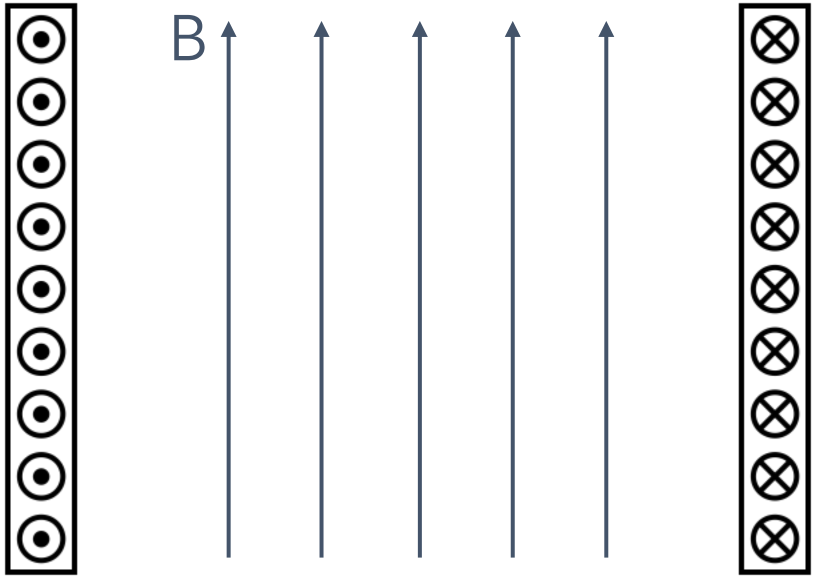

m^3 design

m^3 uses a solenoidal magnet + coaxial copper pickup

No parasitic capacitance

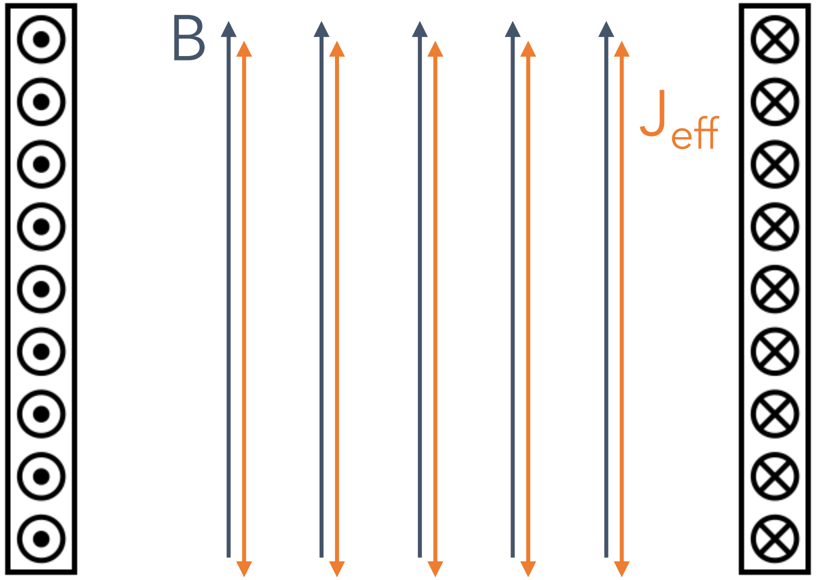

m^3 design

m^3 uses a solenoidal magnet + coaxial copper pickup

No parasitic capacitance

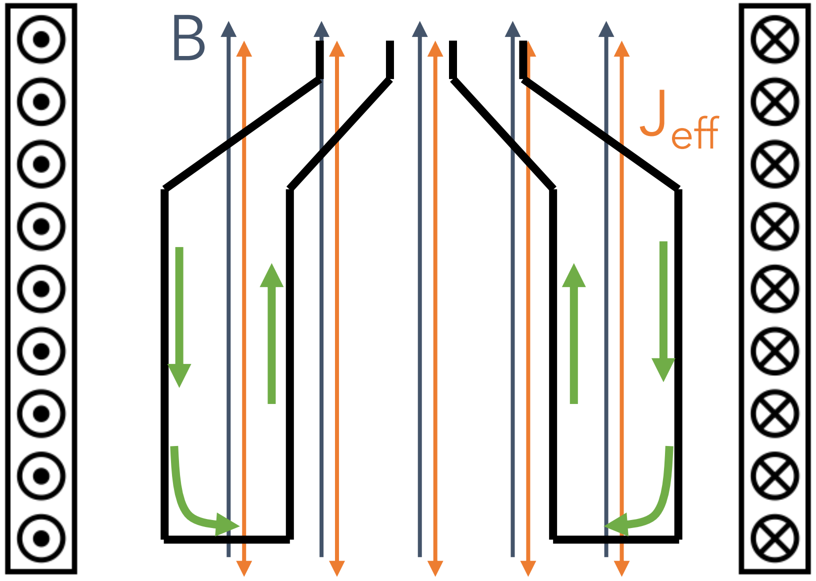

m^3 design

m^3 uses a solenoidal magnet + coaxial copper pickup

No parasitic capacitance

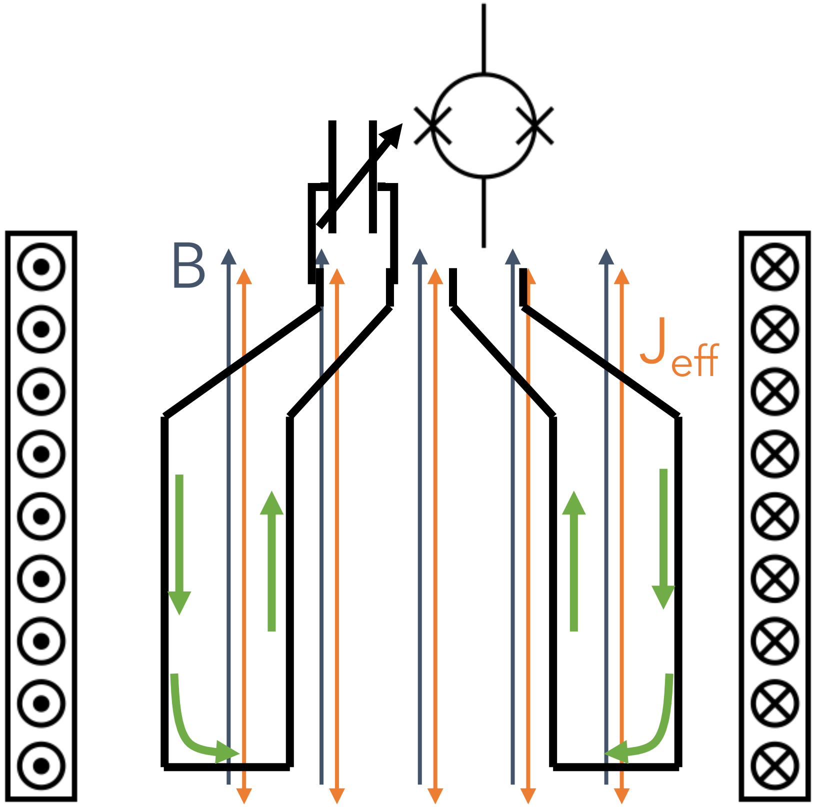

m^3 design

m^3 uses a solenoidal magnet + coaxial copper pickup

No parasitic capacitance

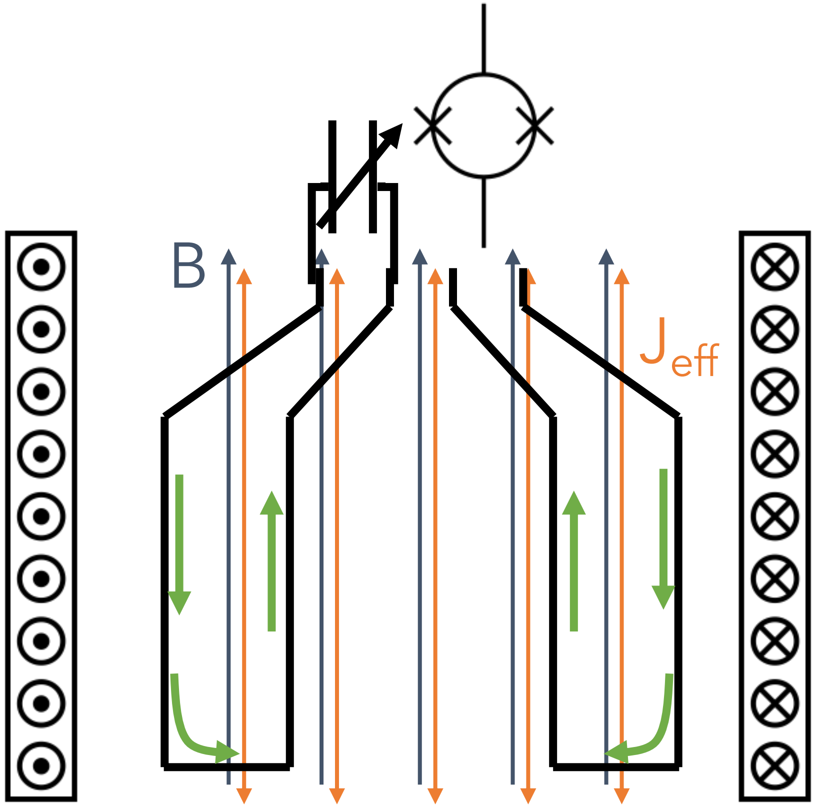

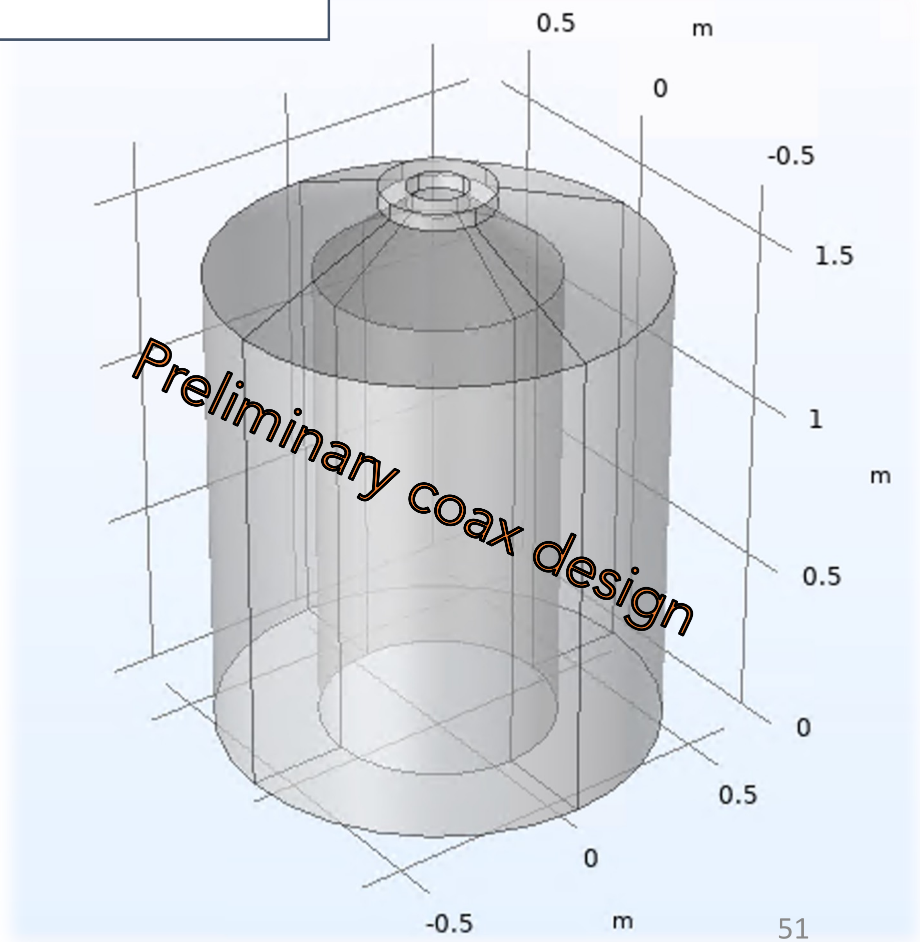

m^3 design

m^3 uses a solenoidal magnet + coaxial copper pickup

No parasitic capacitance

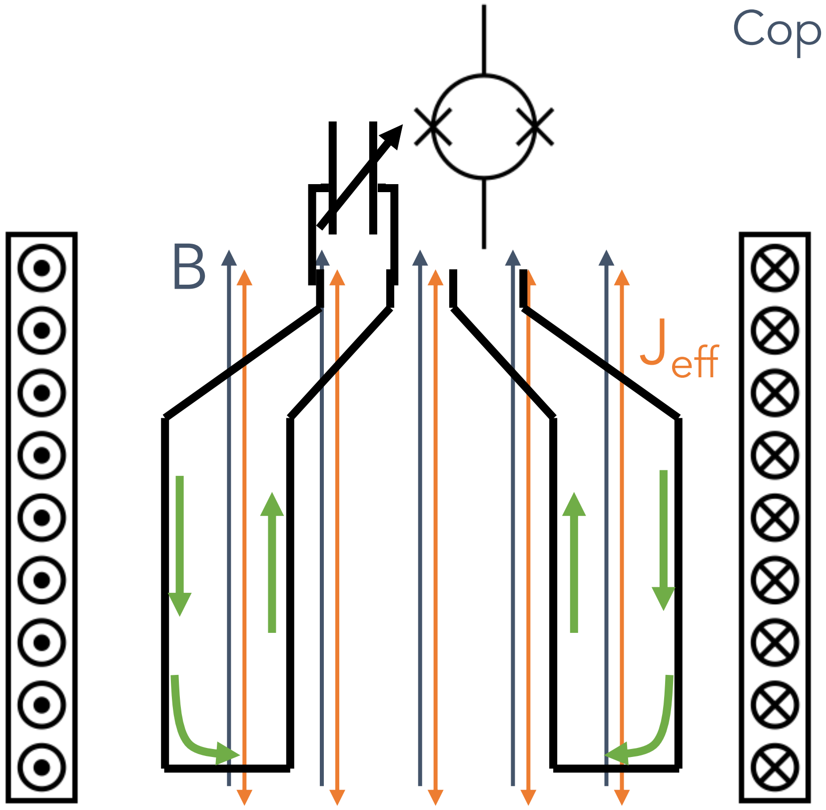

Copper pickup in high B-field region

Coax design favorable for higher frequencies– need careful treatment nevertheless

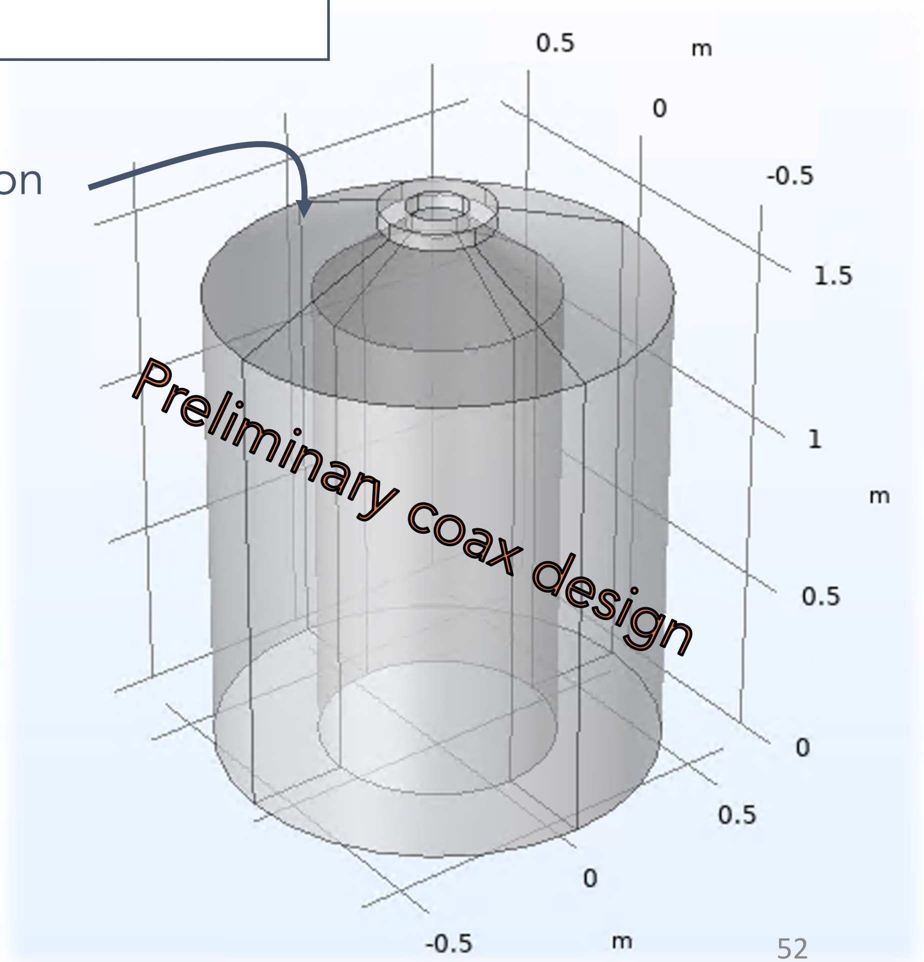

m^3 design

m^3 uses a solenoidal magnet + coaxial copper pickup

No parasitic capacitance

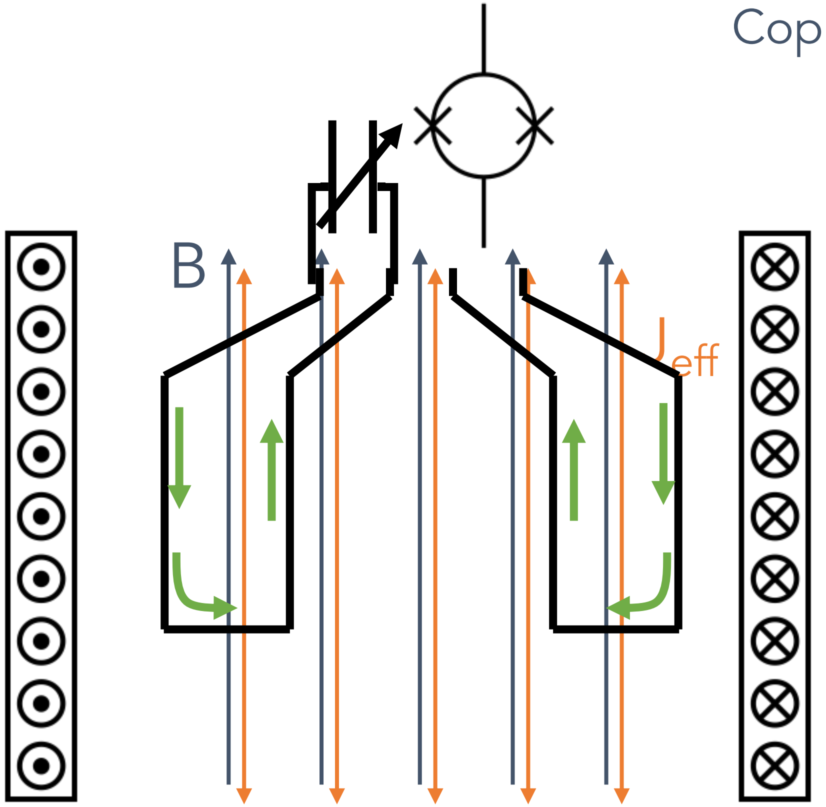

Copper pickup in high B-field region

Coax design favorable for higher frequencies– need careful treatment nevertheless

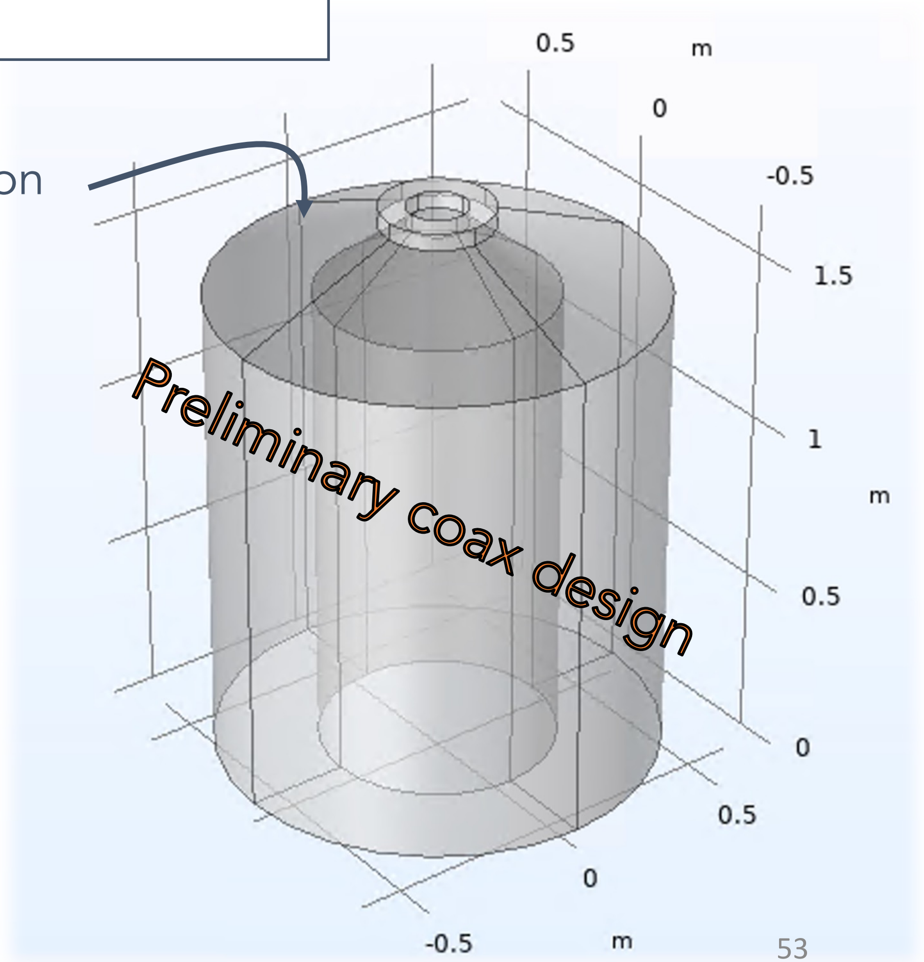

m^3 design

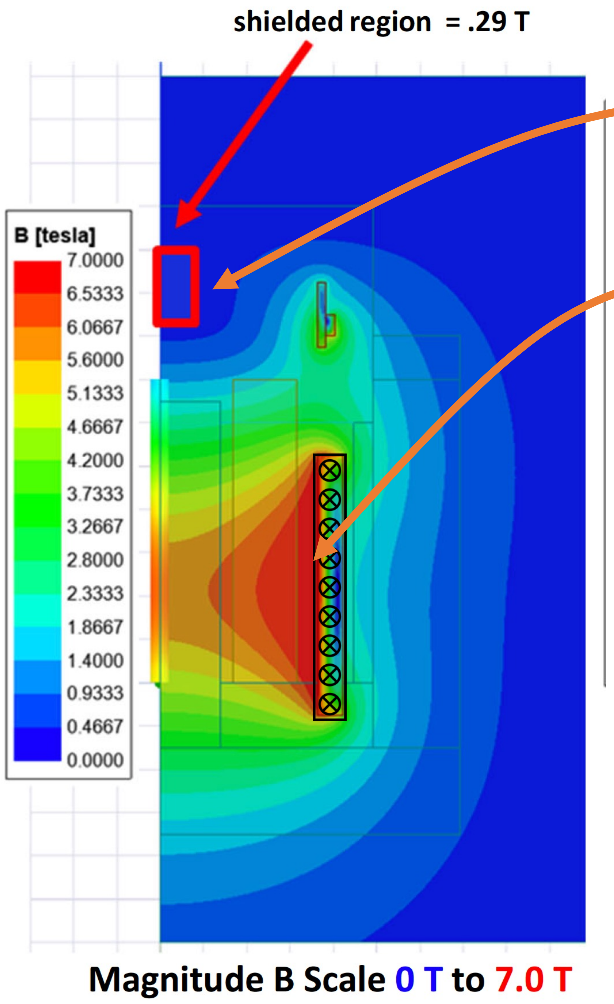

Low B-field region allows for superconducting electronics (less loss)

High B-field region produces larger J_{eff}

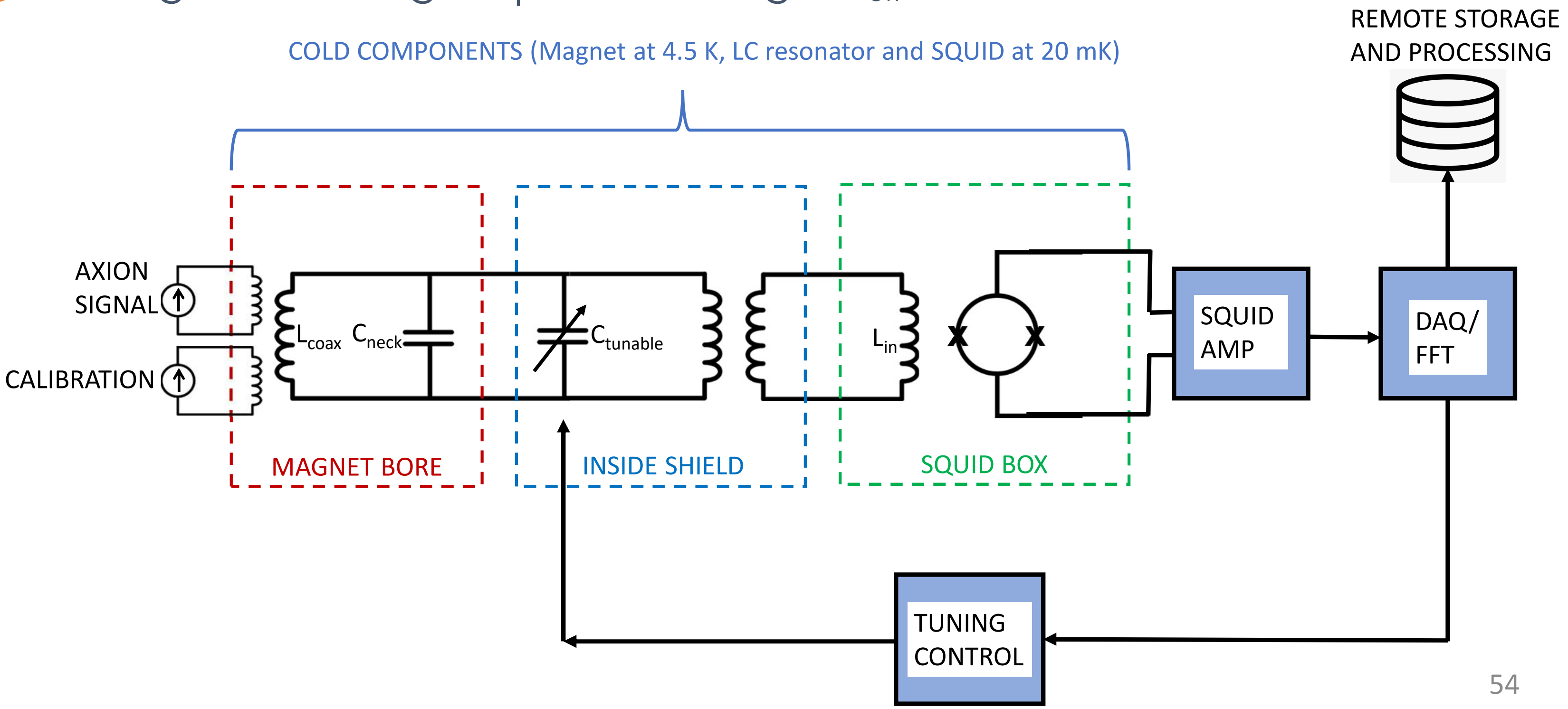

Outline

1. Axions and low frequency haloscopes
2. DMRadio 50L
    1. Overview
    2. Status
3. DMRadio m^3
    1. Overview
    2. Status
4. Outlook, future, & collaboration

DMRadio GUT

RF Quantum Upconverters:

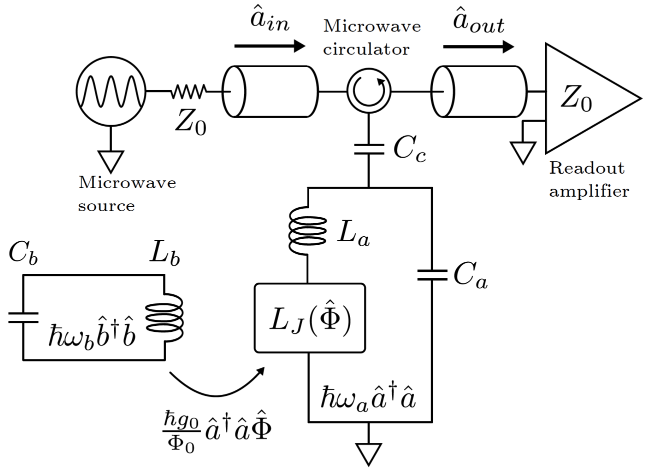

Magnet:

Low vs High T_C still under consideration – significant cryogenic constraints

16 T, 10 m^3

Scan Rate:

$$\frac{d\nu_r}{dt} \approx 41\frac{\text{kHz}}{\text{year}}\left(\frac{3}{\text{SNR}}\right)^2\left(\frac{g_{a\gamma\gamma}}{10^{-19}\ \text{GeV}^{-1}}\right)^4\left(\frac{\rho_{\text{DM}}}{0.45\ \text{GeV/cm}^3}\right)^2$$
$$\times\left(\frac{\nu_r}{100\ \text{kHz}}\right)\left(\frac{c_{PU}}{0.1}\right)^4\left(\frac{B_0}{16\ \text{T}}\right)^4\left(\frac{V}{10\ \text{m}^3}\right)^{10/3}\left(\frac{Q}{2\times10^7}\right)\left(\frac{10\ \text{mK}}{T}\right)\left(\frac{0.1}{\eta_A}\right).$$

Q ~ 20 × 10^6

DMRadio Outlook

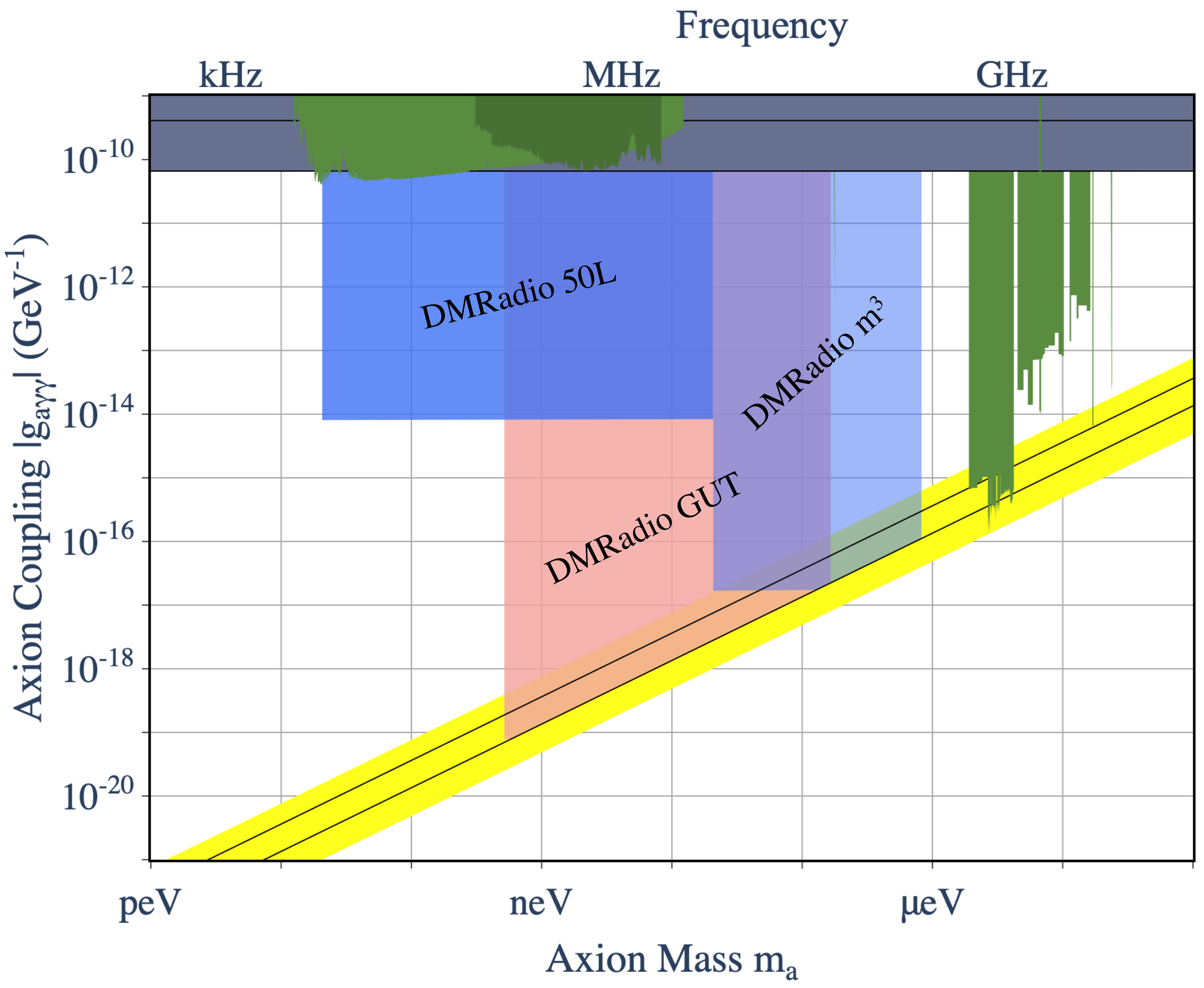

DFSZ @ 0.4 neV < m_a< 800 neV

Projects developed in parallel

$f_a < 10^{19}$ GeV for QCD axion models

Testbed for quantum devices

DMRadio Outlook

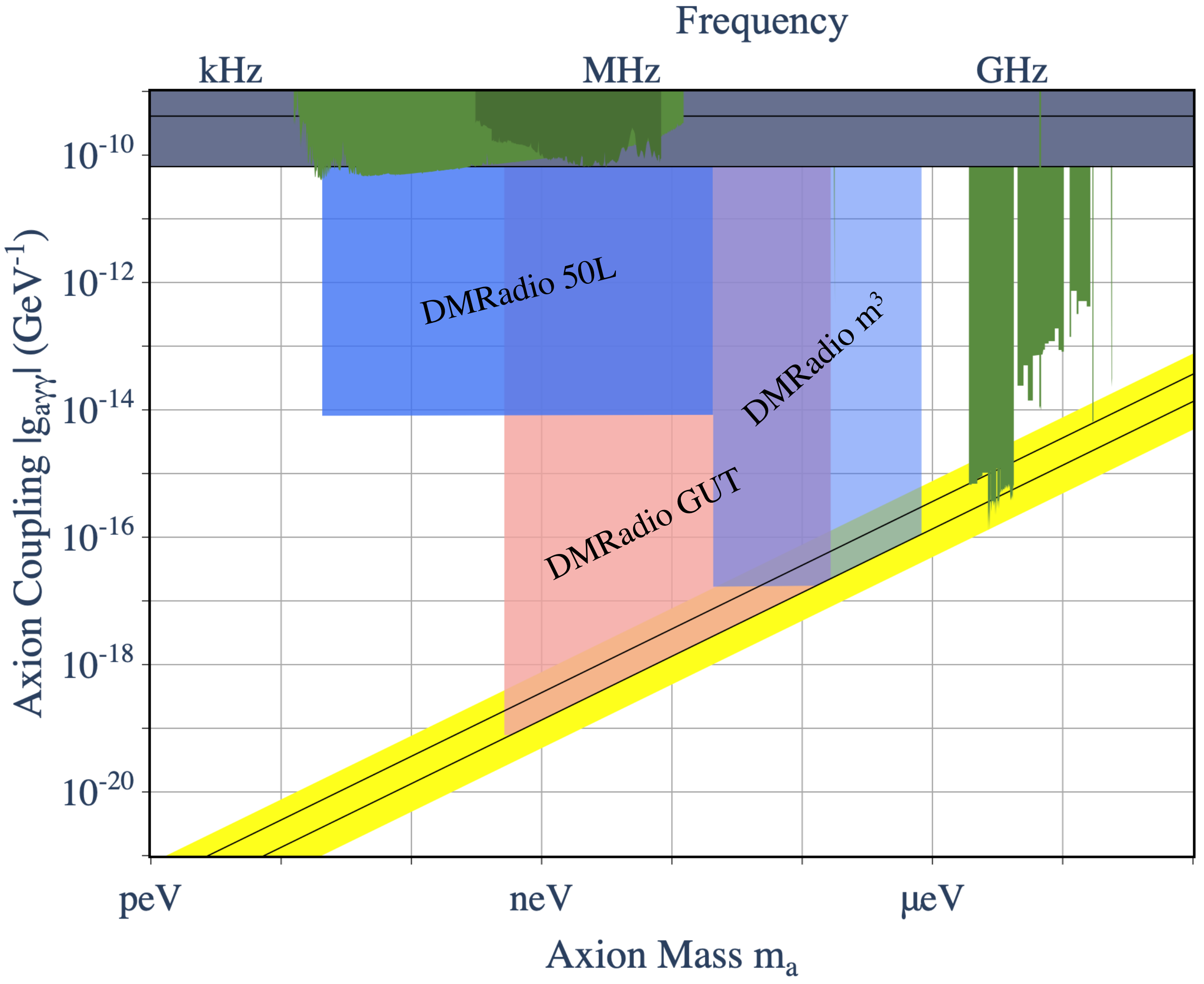

DFSZ @ 0.4 neV < m_a< 800 neV

Projects developed in parallel

f_a < 10^{19} GeV for QCD axion models

Testbed for quantum devices

Publications

50L: coming soon

m^3: arXiv: 2204.13781

GUT: arXiv: 2203.11246

RF Quantum Upconverters:

arXiv: 2210.xxxxxx

DMRadio Collaboration

H.M. Cho, W. Craddock, D. Li, C. P. Salemi, W. J. Wisniewski
SLAC National Accelerator Laboratory

J. Corbin, P. W. Graham, K. D. Irwin, F. Kadribasic, S. Kuenstner, N. M. Rapidis, M. Simanovskaia, J. Singh, E. C. van Assendelft, K. Wells
Department of Physics
Stanford University

A. Droster, A. Keller, A. F. Leder, K. van Bibber
Department of Nuclear Engineering
University of California Berkeley

S. Chaudhuri, R. Kolevatov
Department of Physics
Princeton University

L. Brouwer
Accelerator Technology and Applied Physics Division
Lawrence Berkeley National Lab

B. A. Young
Department of Physics
Santa Clara University

J. W. Foster, J. T. Fry, J. L. Ouellet, K. M. W. Pappas, L. Winslow
Laboratory of Nuclear Science
Massachusetts Institute of Technology

R. Henning
Department of Physics
University of North Carolina Chapel Hill
Triangle Universities Nuclear Laboratory

Y. Kahn
Department of Physics
University of Illinois at Urbana-Champaign

A. Phipps
California State University, East Bay

B. R. Safdi
Department of Physics
University of California Berkeley

Publications

m^3: arXiv: 2204.13781

GUT: arXiv: 2203.11246

Backup Slides

Radiofrequency Quantum Upconverters

LIGO:

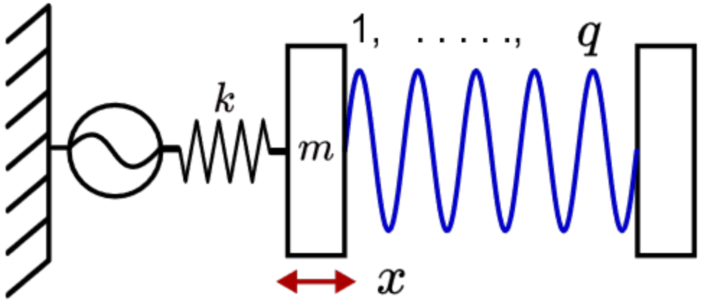

$$\omega_B = \sqrt{\frac{k}{m}} \qquad \omega_A = \frac{2\pi q c}{l(x)}$$

RQU:

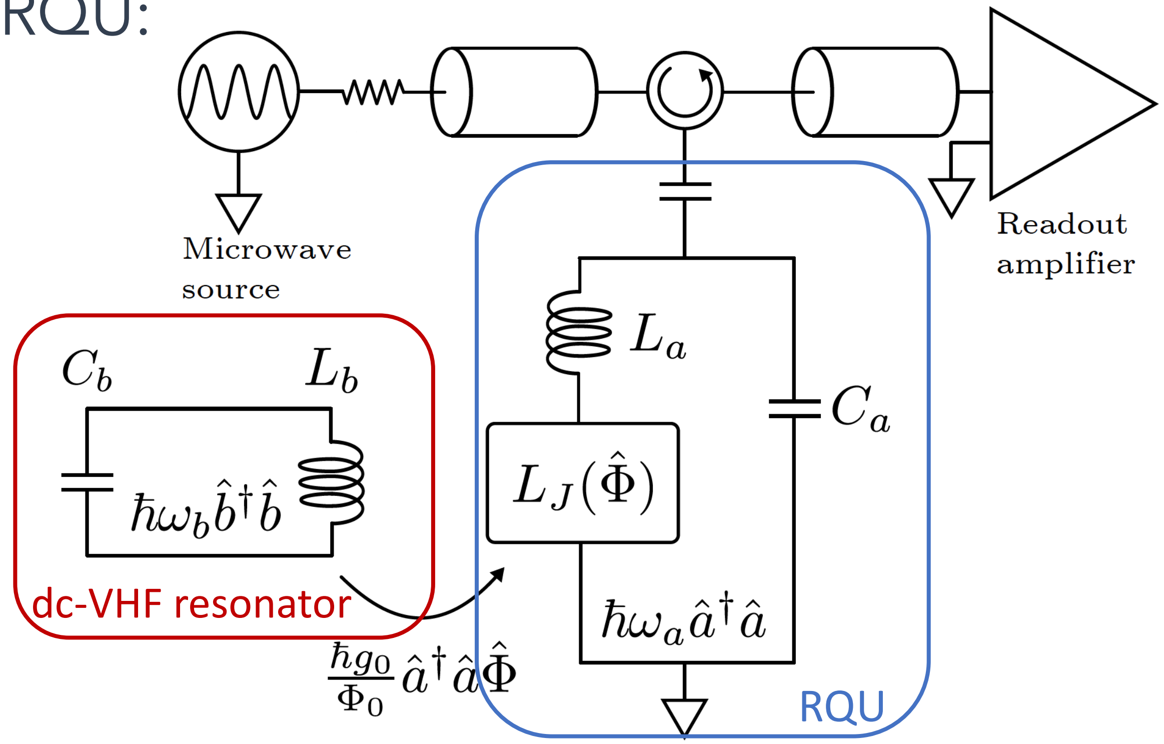

Identical Hamiltonian Formalism:

$$H = \hbar\omega_b \left(b^\dagger b + \frac{1}{2}\right) + \hbar\omega_a \left(a^\dagger a + \frac{1}{2}\right) + H_{\text{int}} \qquad H_{\text{int}} = -\frac{\hbar}{2} F b^\dagger b (a^\dagger + a)$$

Radiofrequency Quantum Upconverters

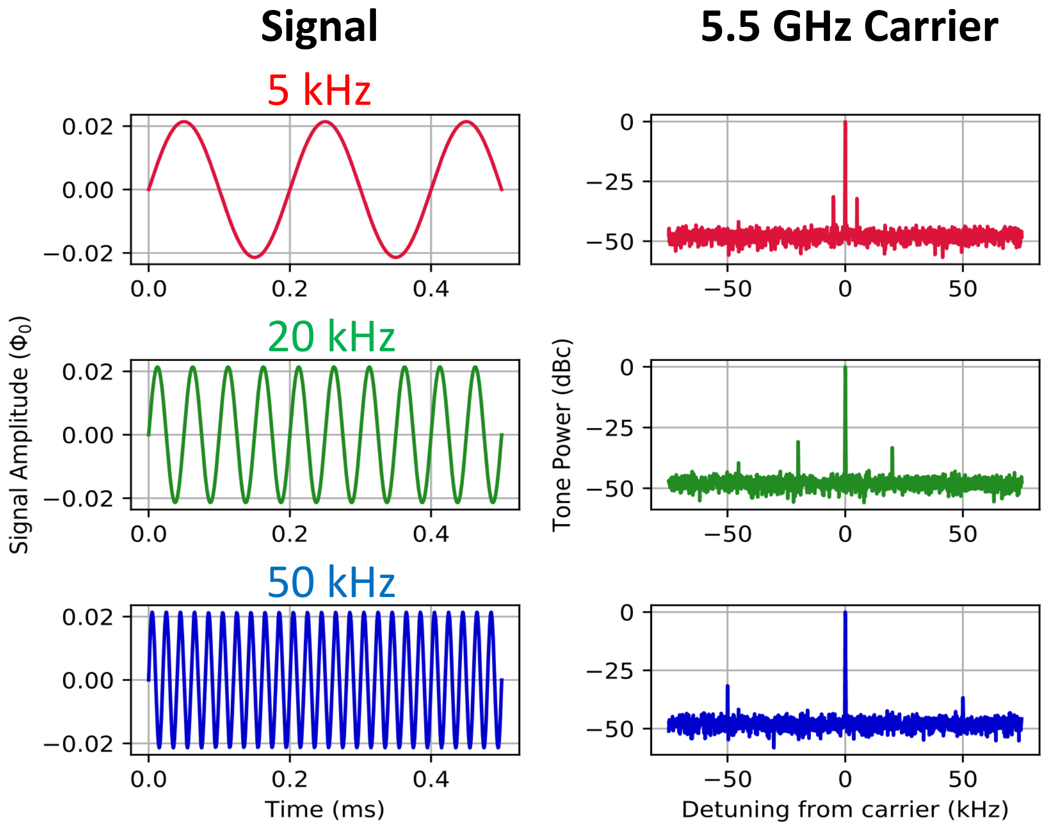

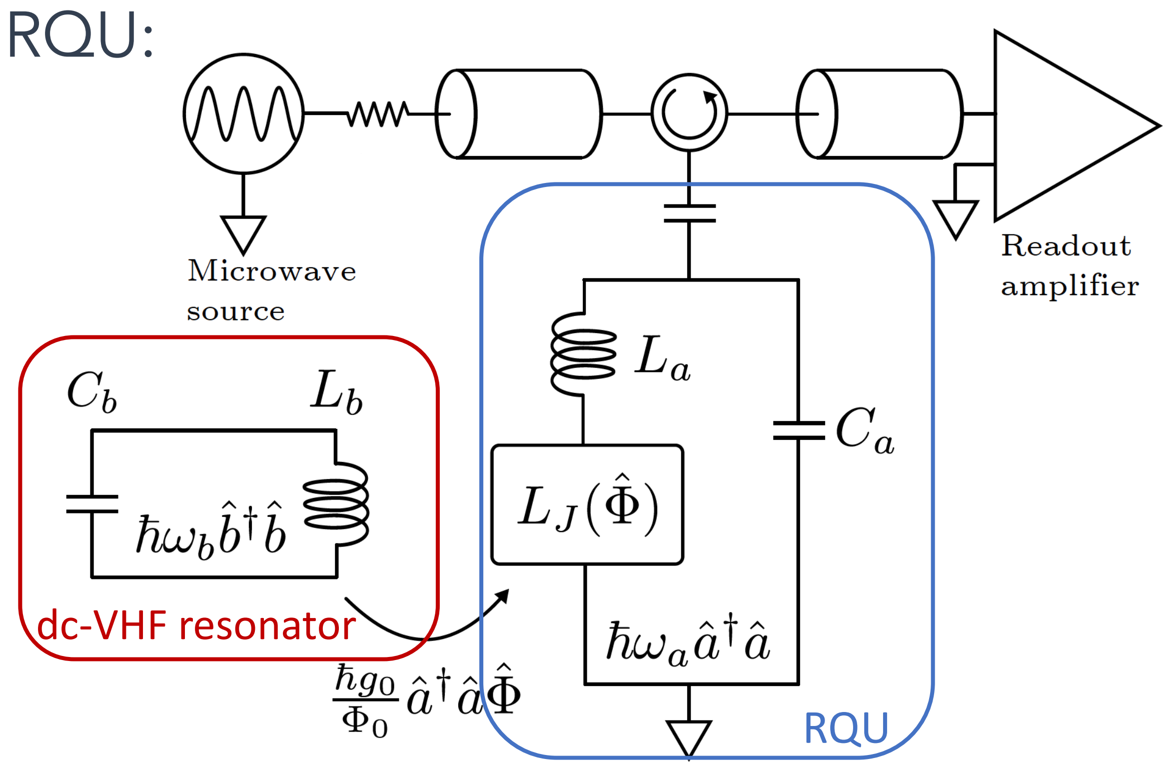

Identical Hamiltonian Formalism:

$$H = \hbar\omega_b \left(b^\dagger b + \frac{1}{2}\right) + \hbar\omega_a \left(a^\dagger a + \frac{1}{2}\right) + H_{\text{int}} \qquad H_{\text{int}} = -\frac{\hbar}{2} F b^\dagger b (a^\dagger + a)$$

m^3 magnet

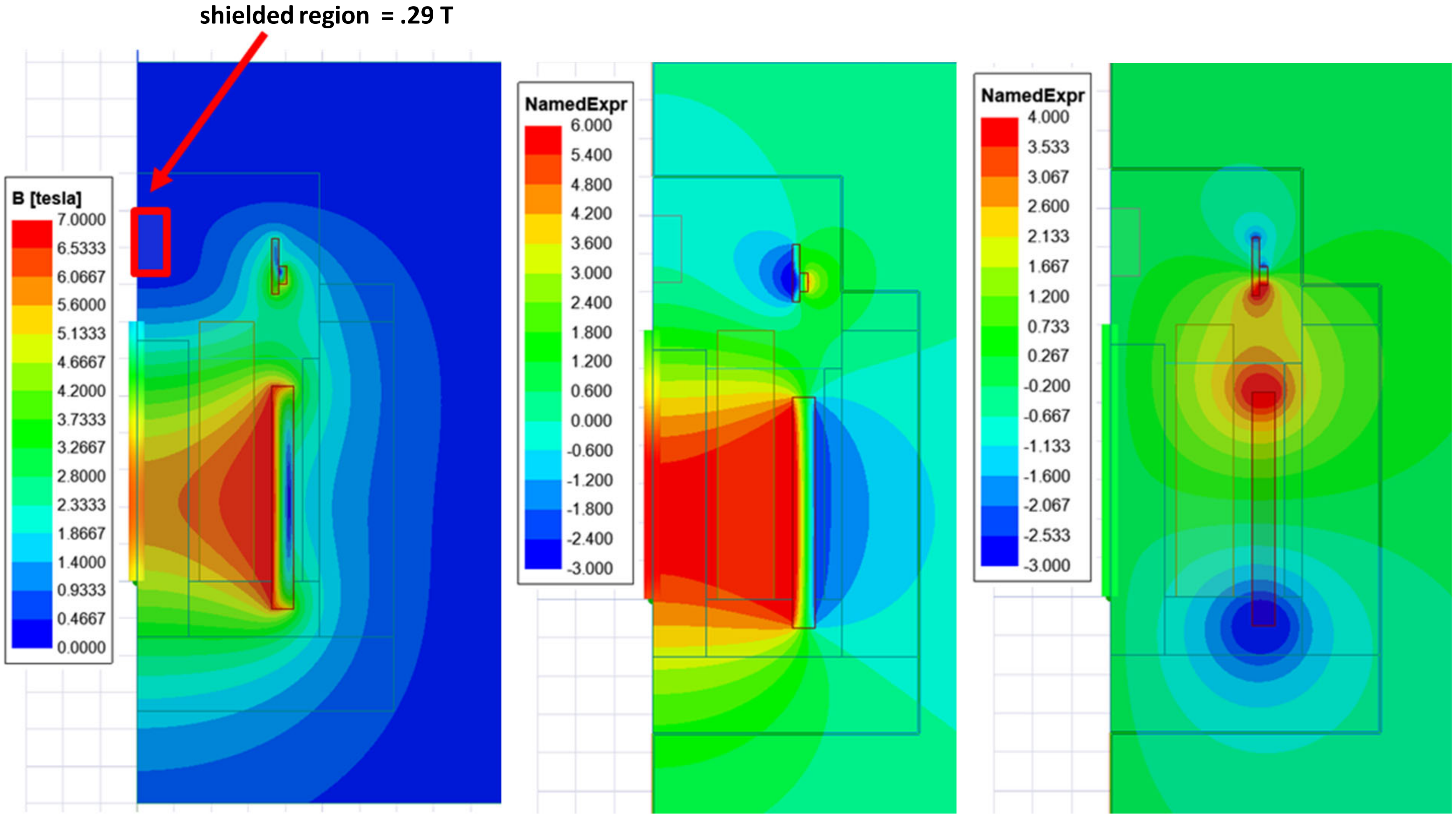

Magnitude B Scale 0 T to 7.0 T **Axial B Scale -3.0T to 6.0 T** **Radial B Scale -3.0 T to 4.0 T**

Misalignment mechanism

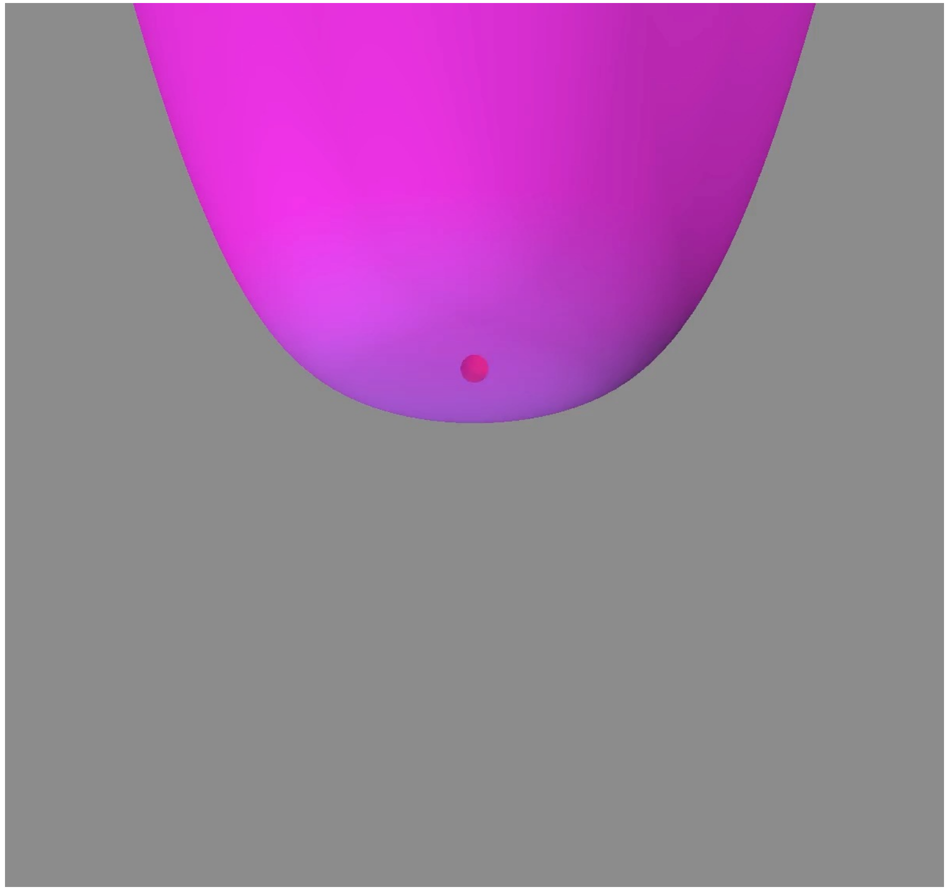

50L details

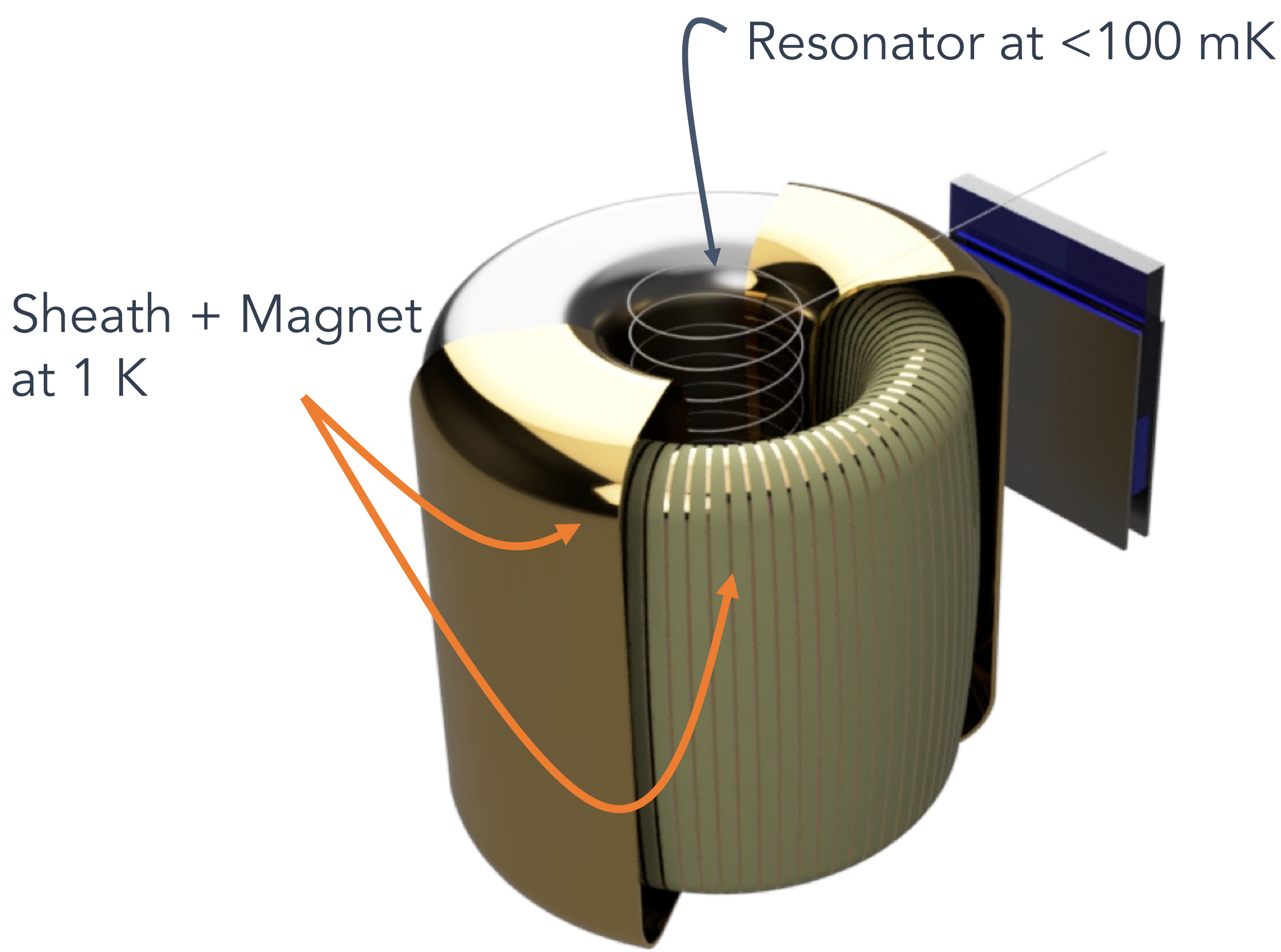

~Coupled energy in resonator vs energy in axion field

Integration time

$$\frac{1}{g_{a\gamma\gamma,\mathrm{min}}} = \frac{c_{\mathrm{PU}}\ B_0\ V^{5/6}\ Q^{1/4}\ \tau_{\mathrm{int}}}{T^{1/4}\ \eta^{1/4}}$$

Amplifier noise temperature, normalized to ½ photon SQL

Physical Temperature